University of Texas at El Paso
DigitalCommons@UTEP

Open Access Theses & Dissertations

2019-01-01

Energy Efficiency and Fatigue Failure on Gears and Bearings for Processing Rebar Steel

Jesus Gabriel Garcia
University of Texas at El Paso

Follow this and additional works at: https://digitalcommons.utep.edu/open_etd

 Part of the Engineering Commons, Oil, Gas, and Energy Commons, and the Sustainability Commons

Recommended Citation
Garcia, Jesus Gabriel, "Energy Efficiency and Fatigue Failure on Gears and Bearings for Processing Rebar Steel" (2019). *Open Access Theses & Dissertations*. 1988.
https://digitalcommons.utep.edu/open_etd/1988

This is brought to you for free and open access by DigitalCommons@UTEP. It has been accepted for inclusion in Open Access Theses & Dissertations by an authorized administrator of DigitalCommons@UTEP. For more information, please contact lweber@utep.edu.

ENERGY EFFICIENCY AND FATIGUE FAILURE ON GEARS AND BEARINGS

FOR PROCESSING REBAR STEEL

JESUS GABRIEL GARCIA

Master's Program in Metallurgical and Materials Engineering

APPROVED:

_____
Devesh Misra, Ph.D., Chair.

_____
David A. Roberson, Ph.D.

_____
Peter Golding, Ph.D.

_____
Stephen L. Crites, Ph.D.
Dean of the Graduate School

ENERGY EFFICIENCY AND FATIGUE FAILURE ON GEARS AND BEARINGS FOR PROCESSING REBAR STEEL

by

JESUS GABRIEL GARCIA

THESIS

Presented to the Faculty of the Graduate School of

The University of Texas at El Paso

in Partial Fulfillment

of the Requirements

for the Degree of

MASTER OF SCIENCE

Department of Metallurgical and Materials Engineering

THE UNIVERSITY OF TEXAS AT EL PASO

August 2019

ACKNOWLEDGEMENTS

I would like to thank to my family and girlfriend for all their support on these 2 years while doing my master's. I also would like to thank to Vinton Steel management for being flexible on my work schedule to achieve my degree. Thanks to UTEP professors with special thanks to my committee for sharing their knowledge, motivation and for guiding me on the process.

ABSTRACT

Steel industry is a major emitter of air pollutants, a leading industrial consumer of water, a minor source of contaminated liquids, a massive producer of solid waste, and a significant source of CO2. The objective on this thesis work is to minimize the greenhouse gas emissions when processing steel. Gears and bearings were evaluated based on their performance when exposed to cyclic stresses. The importance for having a proper set up on rolling mills to increase efficiency for processing rebar steel has been detailed on paper. In contrast, mechanical vibration has been measured on gears and bearings to determine efficiency and to avoid fatigue failure on components. These components are used during hot rolling to plastically deform steel billets and are exposed to cyclic and variable load stresses. It was determined the total amount of energy loss in the form of mechanical vibration, and it was concluded that materials selected on gears and bearings complied with design criteria by failing progressively and not suddenly. Consequently, it was also concluded that energy efficiency on reheating processing is highly affected by fatigue failure on any of the components within the hot rolling processing.

TABLE OF CONTENTS

LIST OF TABLES

LIST OF FIGURES

1. INTRODUCTION

The steel industry is one of the highest energy consumption worldwide. It is also an industry where energy is dissipated during continuous casting process through mold water cooling, spray water cooling and air cooling. The development of continuous casting technology has highly increased energy efficiency, but it faces some serious problems like cracks, inclusions, segregation, oscillation marks, and improper solidification structure distribution (Jha, 2015). The iron and steel industries account for 7% of total global CO_2 emissions (Mahi S., & Sudhari S., 2014). The principal steel producers in the world are China, Japan, the US, India, and Russia. China produces and consumes 50% and 44% respectively of crude steel. Plus, its power consumption is of 9% of whole society (Wu, Su, Li, & Sun, 2019). Mexico is an important iron and steel manufacturer and is the 13th largest steel producer in the world. In 2014, Mexico produced 19 million metric tons (Mt) of crude steel, accounting for 1.16% of the world's crude steel production. It is also the first energy consumption for industrial use representing 14.3% of total industrial consumption (Rojas Cardenas, Hasenbeigi, Sheinbaum, & Price, 2017). The implementation of technologies on steelmaking has lowered significantly the energy consumption. Moreover, the main objective for this thesis paper is to reduce CO_2 gases generated when producing rebar steel by the analysis on wasted energy under certain considerations and scenarios. Energy systems will be modeled to better define the maximum efficiency by the application of thermodynamics laws, mechanical vibration concepts, materials concepts, and materials failure analysis.

2. THERMOMECHANICAL PROCESSING EFFICIENCY

The thermomechanical energy efficiency for producing rebar steel has been optimized to contribute to a friendlier environment in reducing CO_2 emissions. It was modeled to meet the standards of ASTM A615 and A706 on grades 40 and 60; the mechanical properties on yield strength for these grades are 280 MPa and 420 MPa respectively, and a tensile strength of 1.25 times the yield strength or 420 MPa and 620 MPa respectively. Under these standards, the choice and use of alloying elements, combined with carbon, phosphorus, and sulfur to produce the mechanical properties described above, shall be made by the manufacturer. The elements commonly used include manganese, silicon, copper, nickel, chromium, molybdenum, vanadium, columbium, titanium, and zirconium (Standard Specification for Deformed and Plain Carbon-Steel Bars for Concrete Reinforcement, 2018; Standard Specification for Deformed and Plain Low-Alloy Steel Bars for Concrete Reinforcement, 2016). Formula (1) limits the maximum amount of Carbon Equivalent (CE) and for ASTM 706 it should not exceed 0.55% (Standard Specification for Deformed and Plain Low-Alloy Steel Bars for Concrete Reinforcement, 2016). Bars must meet an elongation of between 7 – 14% per every 200 mm in length (Standard Specification for Deformed and Plain Carbon-Steel Bars for Concrete Reinforcement, 2018; Standard Specification for Deformed and Plain Low-Alloy Steel Bars for Concrete Reinforcement, 2016).

$$C.E. = \%C + \frac{\%Mn}{6} + \frac{\%Cu}{40} + \frac{\%Ni}{20} + \frac{\%Cr}{10} - \frac{\%Mo}{50} - \frac{\%V}{10} \qquad \text{Formula (1)}$$

Rebar is produced under the standards of ASTM A615 and A706 for deformed bar and plain round bar. The bar designation numbers start from #3 to #18 and the nominal dimensions of a deformed bar are equivalent to those of a plain round bar having the same weight (mass) per foot (meter) as the deformed bar (Standard Specification for Deformed and Plain Carbon-Steel Bars for Concrete Reinforcement, 2018). Bars diameter range from 0.375” to 2.257” and all their physical properties based on ASTM A706 and A615 are on table below.

Table 1 – ASTM A615 and A706 rebar physical specifications

Bar Designation Number	Diameter, in	Nominal Weight, lb/ft	Nominal Mass, kg/m	Cross-Sectional Area, in^2	Cross-Sectional Area, mm^2
3	0.375	0.376	0.560	0.11	71
4	0.500	0.668	0.994	0.20	129
5	0.625	1.043	1.552	0.31	199
6	0.750	1.502	2.235	0.44	284
7	0.875	2.044	3.042	0.60	387
8	1.000	2.670	3.973	0.79	510
9	1.128	3.400	5.060	1.00	645
10	1.270	4.303	6.404	1.27	819
11	1.410	5.313	7.907	1.56	1006
14	1.693	7.650	11.380	2.25	1452
18	2.257	13.600	20.240	4.00	2581

In electric arc melting of steel, scrap is placed in a furnace, and the furnace uses electrodes to arc on the scrap and melt it. While it is possible to use a single electrode in a DC arc furnace, steel foundries use AC arc furnaces and power companies generate electricity in three opposing phases (Çiftçi B., 2017). The electric arc melting involves charge, melting down, oxidation, and finishing or refining. During the melting processing oxidation of iron, carbon, manganese, and silicon will occur. Phosphorus is controlled and removed after slag is formed on top of liquid steel by tilting the furnace to the slag pot.

2.1 Melting and Reheating Processing Energy

The highest energy consumption on steelmaking occurs during the melting and reheating processing. The amount of energy consumed is highly dependent on the operation procedure for melting mentioned before. The minimum amount of energy that is needed for melting and for obtaining the desired chemistry composition was calculated by the sum of Formulas (2) and (3) where Formula (2) is the amount of energy needed to raise the temperature of steel up to its melting temperature and Formula (3) is the amount of energy needed to rearrange the molecular structure; these are under the assumption of being exposed under constant pressure, and that heat transfer is being delivered at the same rate within its three axes.

$Q = mc_p\Delta T$ Formula (2)

$Q = mL$ Formula (3)

$Q_T = mc_p\Delta T + mL$ Formula (4)

Therefore, Formula (4) is the sum of energy needed to raise steel temperature up to its melting point and the amount of energy needed to rearrange the molecular structure where Q_T is the total energy in kilo joules (kJ). c_p is the heat capacity measured in $\frac{kJ}{kg*°C}$ and it is a measure for the amount of energy needed to raise the temperature to one Celsius degree on one kilogram of mass, ΔT is the temperature change in Celsius degrees ($°C$), m is the mass in kg, and L is the latent heat of fusion or internal energy measured in $\frac{kJ}{kg}$. The heat absorbed by other materials and heat generated by technology is not being taken into consideration.

Consequently, to obtain liquid steel under the following selected conditions with a heat capacity for steel (c_p) taken to be 0.461 $\frac{KJ}{Kg*°C}$, considering an average steel melting point of 1500$°C$ for recycled scrap. If an ambient temperature of 20$°C$ is taken for this analysis, it will give a ΔT of 1480$°C$, a latent

heat of fusion or enthalpy constant (L) for steel of $272\frac{KJ}{Kg}$, and a mass of 1 ton or 1000 kg. The Q_T needed for melting a metric ton (MT) is on Formula (5) under the selected conditions mentioned before.

$$Q_T = mc_p\Delta T + mL$$
$$= 1000\ kg * 0.461\ \frac{kJ}{kg*°C} * 1480°C + 1000\ kg * 272\ \frac{KJ}{Kg}$$
$$= 954{,}280\ kJ = 954.3\ MJ \qquad \text{Formula (5)}$$

The liquid steel is poured into a ladle and billets are produced by continuous casting processing, hence heat is dissipated for solidification 686.8 MJ will be needed as shown on Formula (6).

$$Q_T = mc_p\Delta T + mL$$
$$= 1000\ kg * 0.461\ \frac{kJ}{kg*°C} * (1600 - 700)°C + 1000\ kg * 272\ \frac{KJ}{Kg}$$
$$= 686{,}800\ kJ = 686.8\ MJ \qquad \text{Formula (6)}$$

Another high energy consumption studied is the reheating processing for steel billets. The reheating operation is intended to raise as uniformly as possible the temperature of billet for hot rolling. It is intended to obtain a uniformity temperature on ingot or billet in order to distribute stresses evenly on it when hot rolling. During this process, oxidation and decarburization may also occur on surface due to the ambient conditions to which it is exposed, and it can form carbon monoxide and carbon dioxide. (Roberts, 2017). The reheating process affects yield strength of steel, but it is desirable because it removes superficial defects on ingot surface and increases material toughness and ductility. The maximum efficiency for reheating a billet is given by Formula (6) under the conditions of being at an initial temperature of 20°C and to be reheated to a temperature above its recrystallization point of 980°C giving a ΔT of 960°C, then, for a 1000 kg mass gives 442.6 MJ.

$$Q = mc_p\Delta T = 1000\ kg * 0.461\ \frac{KJ}{Kg*°C} * 960\ °C = 442{,}560\ KJ = 442.6\ MJ \qquad \text{Formula (7)}$$

Therefore, the minimum amount of heat needed for producing a billet is the sum of Formulas 5 and 6 and a total of 1,641.1 MJ needs to be generated (Formula 7). In addition, when reheating processing is needed an extra of 442.6 MJ are added and totals 2,083.7 MJ as on Formula (9). However, the challenge for engineering is to approximate to these numbers by selecting the most efficient procedure along with technology.

$Q_T = 954.6\ MJ + 686.8\ MJ = 1{,}641.1\ MJ$ Formula (8)

$Q_T = 1{,}641.1 + 442.6\ MJ = 2{,}083.7\ MJ$ Formula (9)

2.2 HOT ROLLING PROCESSING AND EFFICIENCY

Hot Rolling is an expensive and very energy consuming operation—hence an attempt is made to keep rolling sequences and schedules to as few steps as possible for giving shape and dimension to the rolled steel. However, hot rolling is not only for giving shape, but it is an important step in steel technology for ensuring correct dimensions, homogeneity of the mass, and quality of the rolled product (Mandal, S. K. 2015). The hot rolling processing comes after billets have been produced and reheated above their recrystallization temperature. Therefore, they are taken out of the reheat furnace and are plastically deformed by applying mechanical forces and shaped by a series of rolling mills as presented on Figure (1).

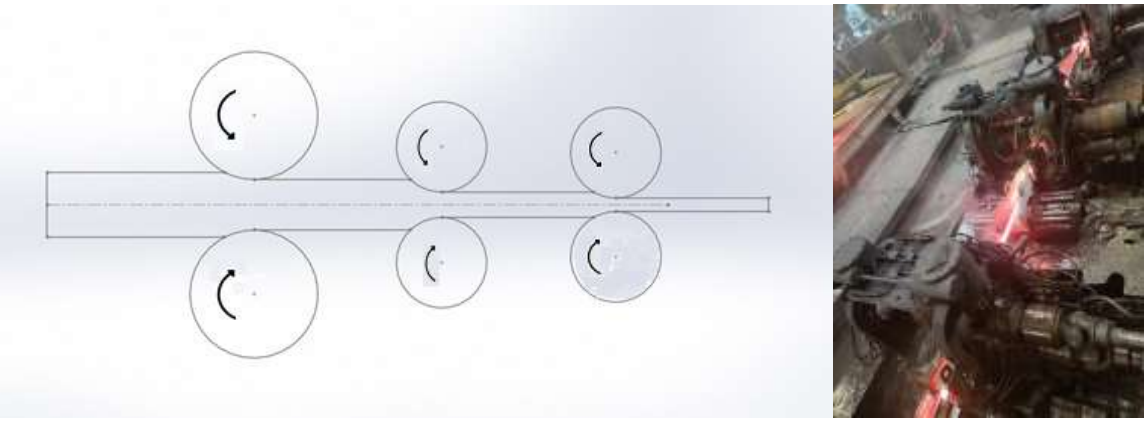

Figure 1 – Rolling mill principle for shaping and strengthening.

The objective when hot rolling is to achieve accuracy on its dimensions, no defects on surface, and to obtained desired mechanical properties. Due to the complex behavior in the industry of the metal flow at high temperatures and the severe plastic deformations in shape rolling, most efforts that have been made so far only rely upon the practical experience gained by operators (Bordonaro, Leardi, Diviani, & Berto, 2018). Subsequently, an analysis to determine efficiency during hot rolling was performed under the following selected considerations for rebar steel processing (Figure 2):

1. Rolls do not present any wear on them and both rolls have the same exact diameter.
2. Rolls and billets are parallel in relationship to floor level.
3. Billet length is at exactly ninety degrees or perpendicular to rolls length, meaning that stresses are going to act the same at any contact point. For proper stress distribution when rolling.

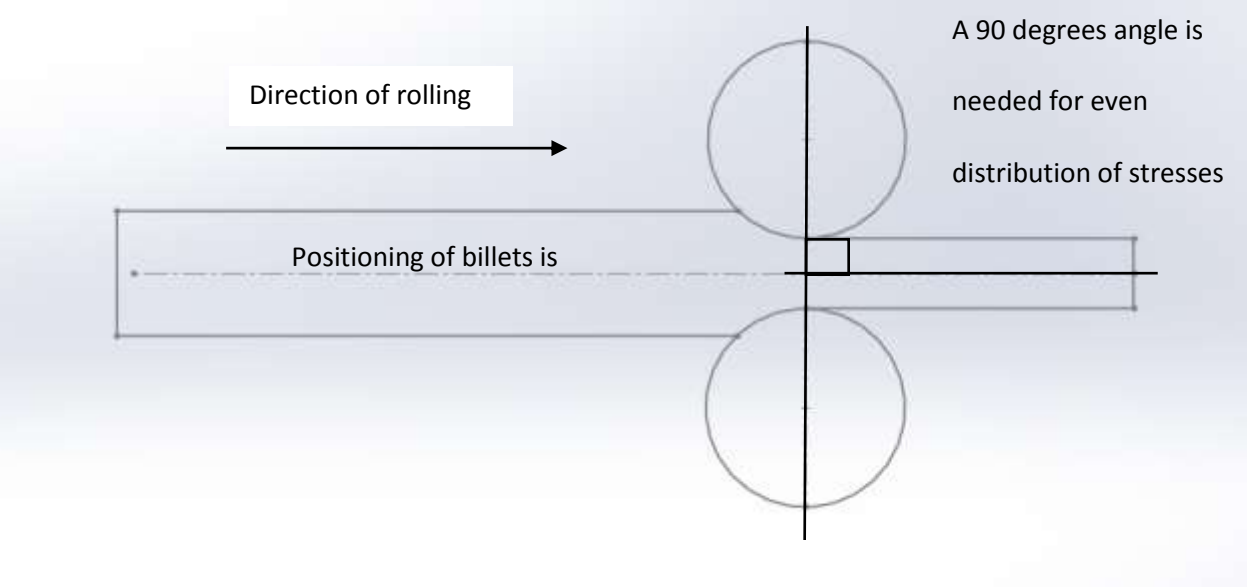

Figure 2 – Rolling direction, and rolls position for maximum stress induced efficiency.

Rolling efficiency is influenced by how effective the rolling sequence is. This process is repeated several times until the bar size diameter is achieved as seen on Figure (1). The stress induced causes grain size elongation and orientation that is parallel to the longitudinal length of the billet or bar; therefore, this processing increases yield strength. The thermal of expansion coefficient is taken for consideration to meet physical requirements of product, and for structural steels a common value

is 12 $\frac{\mu M}{\mathrm{m°C}}$.

The maximum energy efficiency under selected considerations mentioned before to deliver a resultant tension force has been modeled using Solidworks simulation to visualize the stress distribution and dislocation section areas. The highest stress concentration is presented on Figure (3) and occurs when the billet or bar is at the ending contact point with the roll. The highest dislocation section area occurs in a similar way where the highest dislocation is occurring in the area where it is in contact with the roll, as shown on Figure (4).

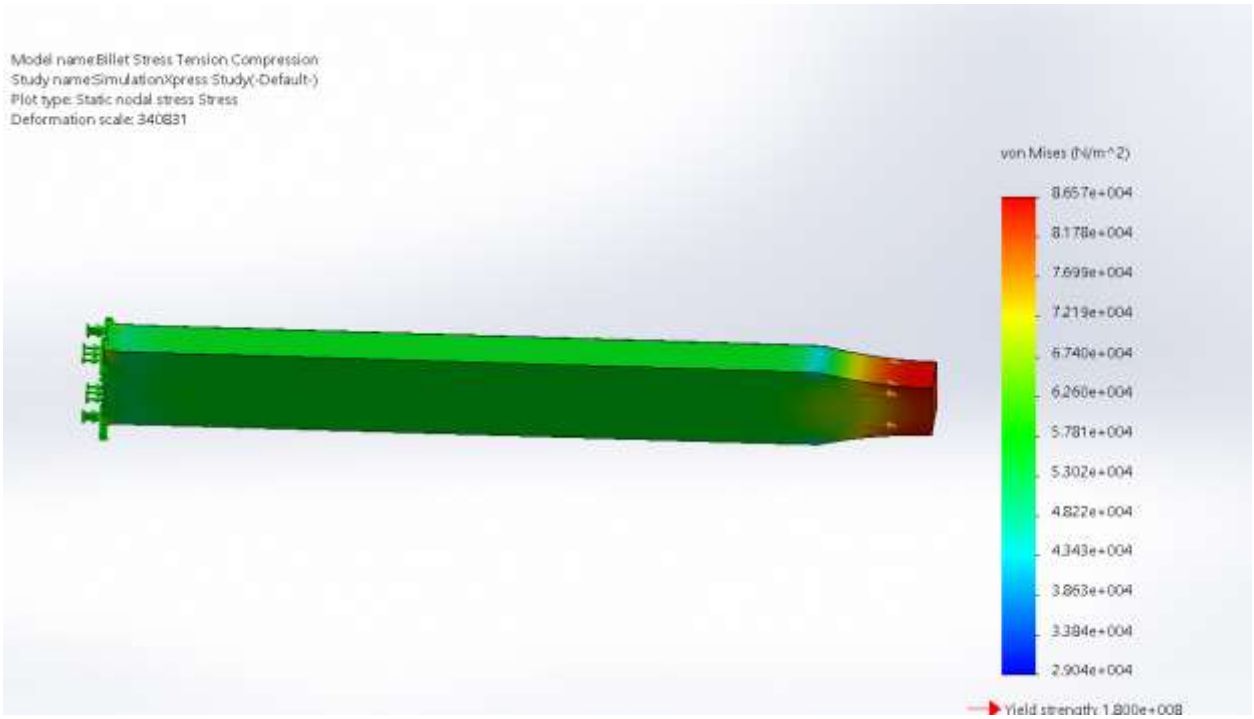

Figure 3 – Billet stress distribution.

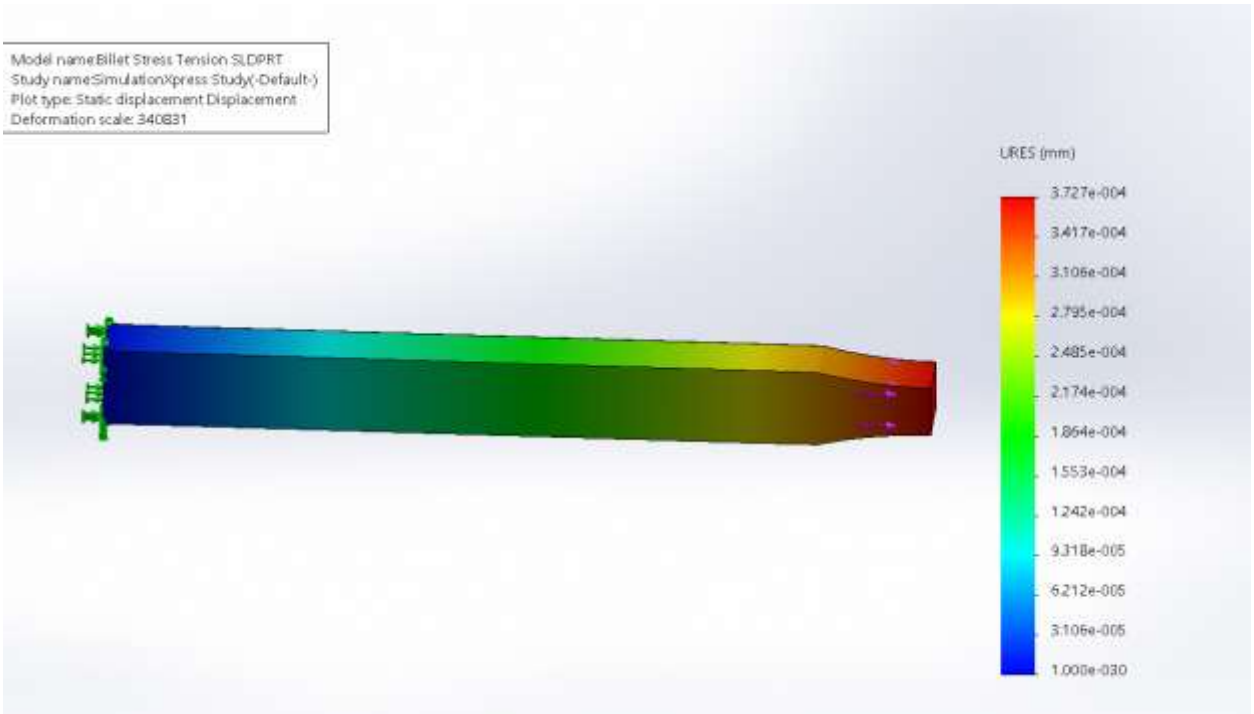

Figure 4 – Billet dislocation section areas.

Billets undergo deformation due to their exposure to external forces that exceed their yield strength. Strain energy theory was applied to approximate the minimum amount of energy needed for hot rolling rebar steel by using Formula (3).

The common structural steel properties are represented on diagram (2) that corresponds to ASTM A36 steel, but in a general sense can represent all common structural steels. At 1600°C, the representative modulus of elasticity and yield strength is 10% (R. H. R. Tide, 2003). For grade 60 at a temperature of 1600°F, its yield strength is 42 MPa, and a modulus of elasticity of 20 GPa is obtained.

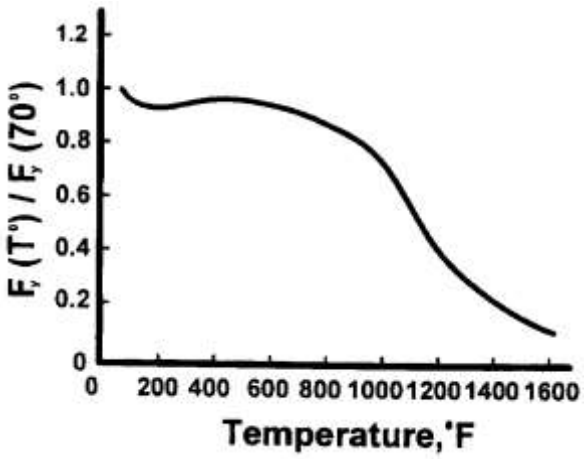

Figure 5 – Representative yield strength – temperature diagram for structural steel A36 (Tide, 2003).

The selected conditions for this analysis is for billets with a square cross section of 5.25” (0.133 m x 0.133 m), a length of 7.47 m, and a mass of 1000 Kg to maintain consistency in comparisson with previous calculations.

Figure 6 - Billet physical dimensions

Consequently, the cross section area (CSA) was divided into multiple segments to calculate the axial forces needed to start deforming on rolling processing by taking the maximum allowable stress or yield stress (σ_y) of 42 MPa for a temperature of 900°C. Then, after the CSA forces were gradually calculated, the minimum total amount of energy needed for plastic deformation was calculated on Table (2) based on its change in length.

Table (2) – Cross section areas (CSA) ranging from an initial 0.0177 m^2 to lower CSA of 0.000129, which is equivalent to rebar #4 area, and their respective axial forces needed to initiate deformation on billet with a yield strength of 42 MPa at 900°C.

	Cross Section Area in m^2	**Axial Force Needed (N)**	**Length, (m)**	**Total Energy Accumulated, (J)**
		$\sigma_y A = F$		$U = F \times \Delta d$
		$42\ MPa * A = F$		
Initial Billet	0.017700	743,400	7.47	0
	0.016000	672,000	8.3	579,852
	0.015000	630,000	8.8	949,452
	0.014000	588,000	9.4	1,345,452
	0.013000	546,000	10.2	1,771,914
	0.012000	504,000	11.0	2,233,914
	0.010500	441,000	12.6	3,025,914
	0.009500	399,000	13.9	3,609,492
	0.008000	336,000	16.5	4,648,992
	0.006000	252,000	22.0	6,496,992
	0.003500	147,000	37.7	10,456,992
	0.000900	37,800	146.7	26,472,992
Rebar #10	0.000819	34,398	161.2	27,021,300
	0.000700	29,400	188.6	27,963,780
	0.000500	21,000	264.0	30,181,380
	0.000300	12,600	440.0	33,877,380
	0.000200	8,400	660.0	36,649,380
Rebar #4	0.000129	5,418	1023.3	39,700,729

Therefore, the highest axial force needed during hot rolling processing occurs when its cross-section area is at its maximum value or at the beginning. In this scenario, it is 743.4 KN with a CSA of 0.0177 m^2. Subsequently, when the CSA is lower the speed for rolling speed increases to increase productivity on steel mills.

The highest energy consumption rate occurs at the beginning of rolling. On Figure 7 the energy accumulated by small reductions on cross section areas is graphed. Thus, an amount of between 13 to 40 MJ for rolling processing are needed. In addition, its behavior was obtained as a logarithmic Formula as a function of bar length in meters. Between 33% to 50% of total energy depending on product that is being produced occurred when billet length has been elongated to 25 m in length as marked on red section area below.

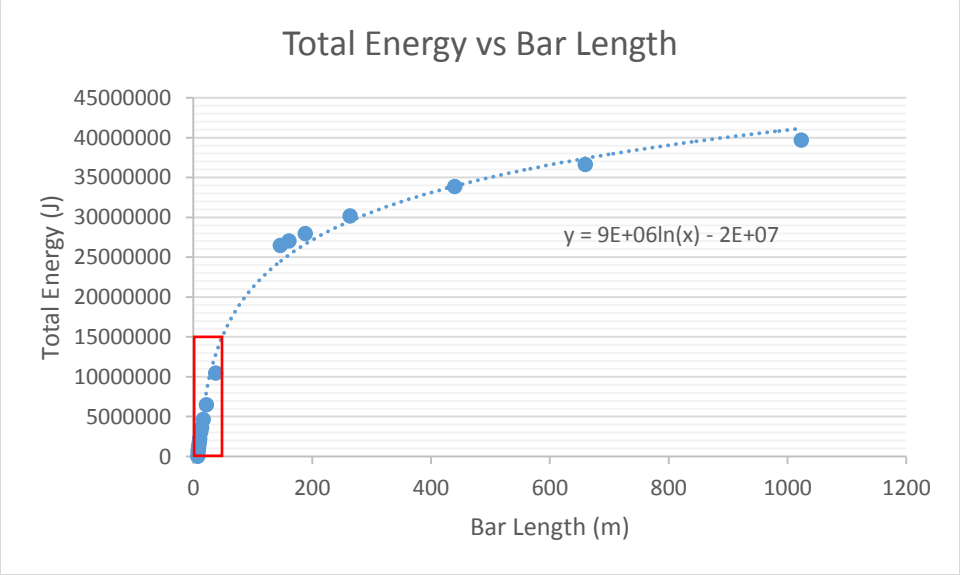

Figure 7 - Total energy accumulated for Cross Section Reduction (CSA) as a logarithmic function of bar length.

The case in which misalignment between rolls or between two rolling mills exists was simulated under a 2° of misalignment scenario. The continued misoriented acting force against machinery is going to cause failure fatigue on mechanical drive train components that will be discussed on next chapter due to the increase in stress and impacts received on rolls. The distribution on residual stresses between top and bottom are shown on Figures (8-9). In contrast, there exists a higher stress concentration on top section area than on bottom. Subsequently, the dislocation or displacement will be more predominantly on top section as presented on Figure (10).

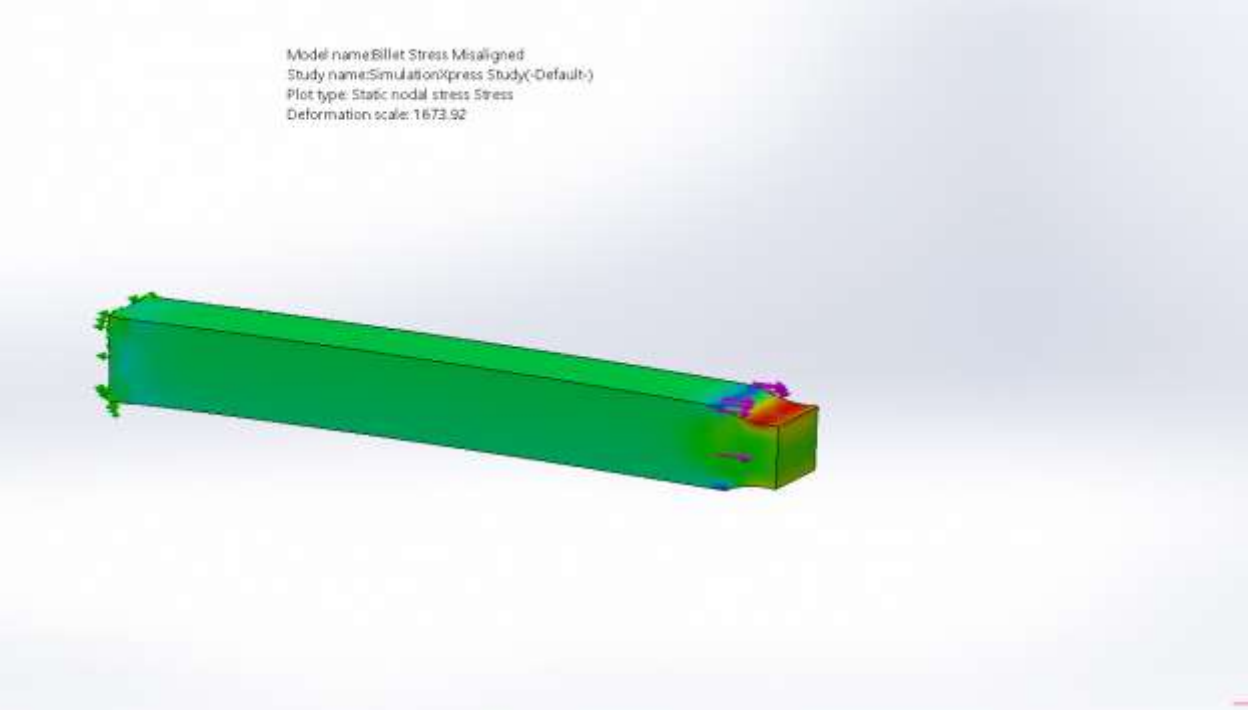

Figure 8 – Billet top view under a higher stress concentration.

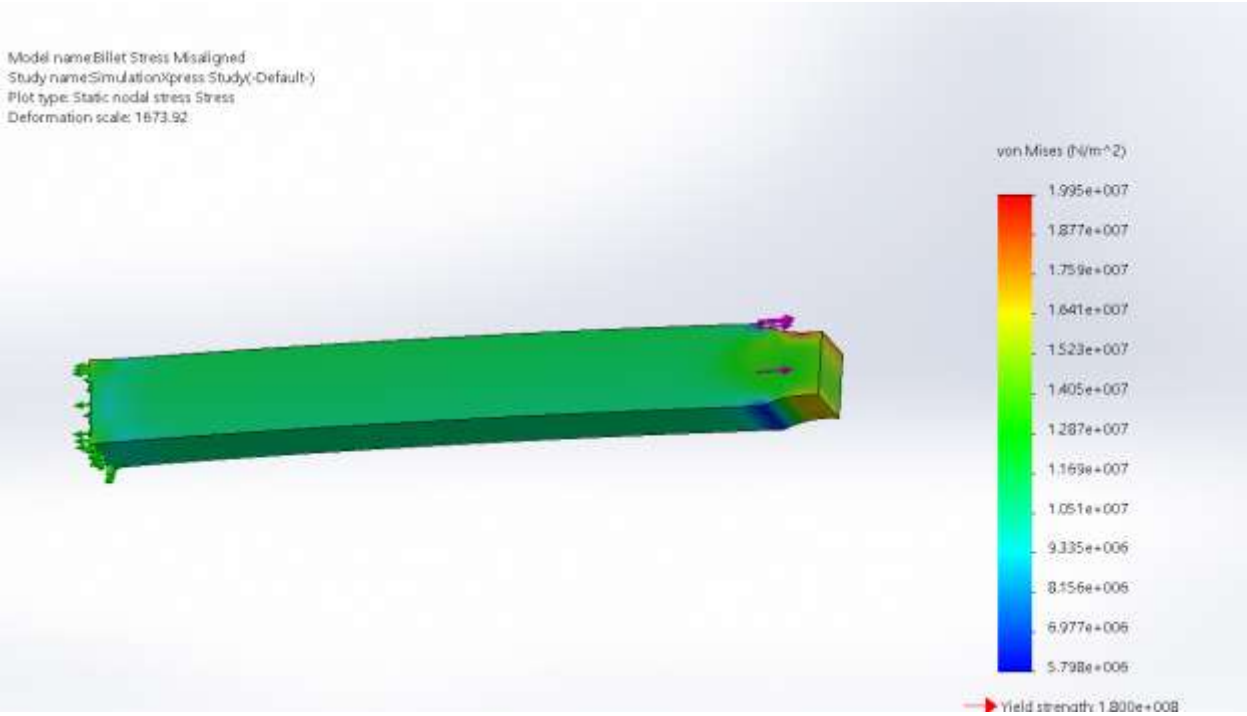

Figure 9 – Billet bottom view under a lower stress concentration.

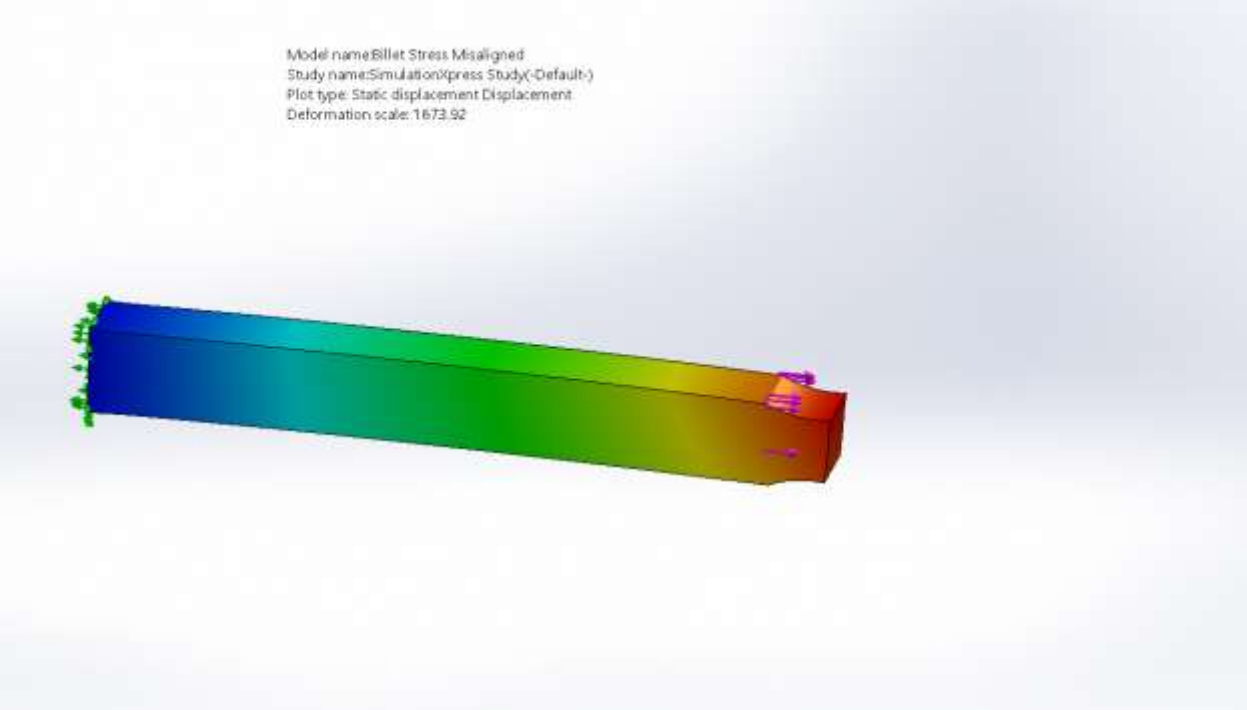

Figure 10 – Dislocation billet model

The highest amount of misoriented force occurs at the beginning of rolling when cross section area is at its highest value as calculated on Table (3). By comparing Table 2 and Table 3, it can be concluded that there exists a minimum energy saving of 25,000 J per every billet 1000 kg that is hot rolled.

Table 2 – Force disoriented under a 2° misalignment between rolls and bar.

2° Misalignment					
Cross Section Area in m^2	**Axial Force Needed (N)**	**Force Misoriented (N)**	**Length, (m)**	**Resultant Force (N)**	**Total Energy Accumulated in Joules, (J)**
0.017700	743,400	26,019	7.47	743,855	0
0.016000	672,000	23,520	8.3	672,411	580,207
0.015000	630,000	22,050	8.8	630,386	950,033
0.014000	588,000	20,580	9.4	588,360	1,346,276
0.013000	546,000	19,110	10.2	546,334	1,772,999
0.012000	504,000	17,640	11.0	504,309	2,235,281
0.010500	441,000	15,435	12.6	441,270	3,027,766
0.009500	399,000	13,965	13.9	399,244	3,611,703
0.008000	336,000	11,760	16.5	336,206	4,651,839
0.006000	252,000	8,820	22.0	252,154	6,500,971
0.003500	147,000	5,145	37.7	147,090	10,463,395
0.000900	37,800	1,323	146.7	37,823	26,489,202
0.000819	34,398	1,204	161.2	34,419	27,037,846
0.000700	29,400	1,029	188.6	29,418	27,980,903
0.000500	21,000	735	264.0	21,013	30,199,861
0.000300	12,600	441	440.0	12,608	33,898,124
0.000200	8,400	294	660.0	8,405	36,671,821
0.000129	5,418	190	1023.3	5,421	39,725,038

Therefore, the difference between proper alignment and a misalignment of 2° is 25 kJ. The highest impact will be on the misoriented force that is acting against components dealing with uneven loads and impacts and this force is 3.5% of the axial force that is needed for rolling. In addition, product quality is affected by the inducement of uneven compressive stresses on billet or rebar.

3. PROCESSING EQUIPMENT AND FATIGUE FAILURE ENERGY ANALYSIS

In contrast, due to the high amount of load that is needed as calculated on Table (2) for rolling and plastically deform a billet, it is of importance to maintain the mechanical system at best conditions to avoid any misoriented force with the potential to cause any failure. The mechanical properties to be taken into consideration for materials selection of equipment used in steel industry are based on thermal stability, creep resistance, strength, hardness, and corrosion resistance. Lubrication on gears and bearings is highly important to prevent a premature failure. Lubricant is essential for all gearing and bearings subject to measurable loadings, and even for lightly or negligibly loaded instrument gearing, it is needed to reduce friction (Sadegh & Worek, 2018).

The reliability on gears and bearings depends on both their hardness values to avoid any surface defect that can initiate failure on material, therefore, when abrasive particles get into gears and bearings, they will resist more against inclusions and wear.

Rolling mills are used to deliver the necessary force for shaping and form rebars, however, they are exposed to not desired conditions that with time efficiency is affected. A typical gear train system used for rolling processing consists of a motor coupled to a speed reducer gearbox with an output coupled to a differential gearbox as seen on Figure (11), therefore, because of the number of components and contact points to deliver work, any imperfection within the system has the potential to initiate and propagate failure.

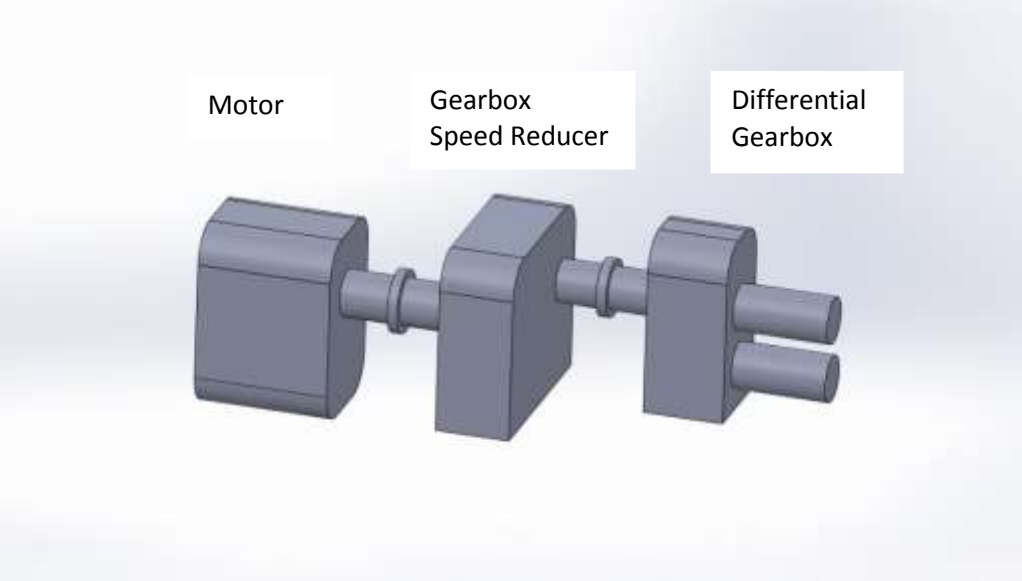

Figure 11 – Rolling mill gear train system.

Figure 12 - Rolling mill uncoupled ≅ size 2.0 m x 2.7 m

Hence, Figure 12 is a rolling mill with an approximate capacity to exert an axial force of 300 kN; it is used when it is between 4% to 25% from the final length of elongation and based on Table (2) it corresponds to rolling mills where energy consumption rate is higher. Inefficiency on a system will initiate failure on a material. Mechanical properties of equipment must be exceeded to withstand higher loads to prevent failure; however, failure occurs after a period of time generated by fatigue conditions.

Mechanical energy is transmitted by gears that are widely used to generate motion and torque needed for rolling mills that are subjected to thermal and variable load stresses that in the long term their failure mode will be of fatigue, impact, wear, and stress fracture; these are caused by tooth bending, abrasive particles, shear stresses, or when yield strength has been exceeded (Metals Handbook, 1978).

Consequently, XRF analysis was performed on a gear tooth fracture, and chemistry composition results were close to 41XX steel series; these steels have a composition of Cr 1.0% and Mo 0.25% and yield strength values between 740 MPa to 1860 MPa that depend on tempering temperature as shown on Table 4 (Karassik, 2008).

Table 3 – Tempering temperature and mechanical temperature.

Tempering temperature		Tensile strength		Yield strength		Elongation in 50 mm or 2 in, %	Reduction in area, %	Hardness		Izod impact energy	
°C	°F	MPa	ksi	MPa	ksi			HB	HRC	J	ft · lb
205	400	1980	287	1860	270	11	39	520	53	20	15
315	600	1760	255	1620	235	12	44	490	49.5	14	10
425	800	1500	217	1365	198	14	48	440	46	16	12
540	1000	1240	180	1160	168	17	53	360	39	47	35
650	1200	1020	148	860	125	20	60	290	31	100	74
705	1300	860	125	740	108	23	63	250	24	102	75

Typical hardness values for steels used on gears and description are on Table (5) where a hardness value higher than 50 HRC is acceptable for this type of industry. It is important to recall that the difference in hardness between two gears that are in contact affects system life by inducing

compressive residual stresses during operation (Zaretsky, Parker & Anderson, 1967). Typical gear hardness values are on Table (5) where in this case, a value of 58 in HRC scale is acceptable based on the high amount of work needed for rolling.

Table 4 - Hardness values on Rockwell C scale for common steels used on gears (Sadegh & Worek, 2018).

Rockwell C	Machinability	Comments
24	Easy	Very low hardness
24 - 32	Moderately Hard to cut	Medium hardness; good load capacity
32 – 37	Hard to cut	High hardness; excellent load capacity
38	Very hard to cut	High hardness; load capacity excellent
51	Requires grinding to finish	Very high hardness; wear capacity good
58	Requires grinding to finish	Full hardness, very high load capacity
65 - 70	May be surfaced hardened after final machining	Super hardness; obtained by nitridizing, Very high load capacity.

Life expectancy on gears and bearings materials depends on conditions to which they are exposed such as load, temperature, rpm, and ambient will define its duration. The surface material on gears and bearings will tend to deteriorate and to wear during its normal operation, and due to the exposure against abrasive particles, and uneven thermal and load stresses distribution, a high hardness on surface is necessary to avoid any crack initiation and to prevent it from wear.

Bearings are critical components in the operation and their reliability is highly important, they are designed to withstand static and dynamic loads. Their most common failure modes are wearing, electrical pitting, fretting, corrosion, indentation, elevated temperature, cracking and fracturing. These can be generated by; vibration, low or without lubrication, abrasive materials, or by an excessive force applied. A commonly accepted minimum surface hardness for most bearing components is 58 HRC (Metals Handbook, 1978). AISI 440C stainless steel which is suited for moderately corrosive environments has a maximum hardness value of 62 HRC. The drawbacks for this type of steel is that it has a maximum working temperature of 175C compared to 315C on CBS1000M. The 52100 steel

through hardened is widely used for ball bearings, and 8260 for roller bearings. The carbide structure on 440C is coarser, making it softer than the 52100 series steel, and fracture toughness is about one half than 52100 (Metals Handbook, 1978). The life and reliability of the system cannot exceed the life and reliability of the lowest lived component in the system (Zaretsky & Branzai, 2017). Moreover, XRF for chemistry comoposition on an outer race bearing was obtained and results were closed to 52100 steel composition.

Therefore, mechanical vibration has been measured to evaluate the actual conditions on gears and bearings when they are exposed to fatigue scenarios. In a total plant performance mode, predictive technology can be used to accurately measure the effectiveness and efficiency of all plant functions, not just machinery. The data generated by regular evaluation can isolate specific limitations in skill levels, inadequate procedures, and poor management methods as well as incipient machine or process system problems (Outinen & Mäkeläinen, 2004).

3.1 Introduction to Mechanical Vibration

Vibration is defined as small oscillations about some equilibrium point. The main characteristics of vibration are amplitude and frequency (Whitaker & Benson, 2001). A vibrating system of any kind that is driven by and is completely under the control of an external source of energy is in a state of forced vibration. (3) Vibration on a mechanical system is a sign of inefficiency. Systems under forced vibration generate a frequency that defines the type of external and not desired forces that are acting against it.

Any force acting at an undesired direction on a mechanical system will generate vibration as a form of energy, and this is directly proportional to the efficiency of the system. In addition, if this vibration exceeds the permissible stress intensity on material which is usually 150 $MPa\sqrt{m^2}$will cause failure.

According to Moble (2014), it states that vibration analysis is predicated on two basic facts: (1) all common failure modes generate a vibration frequency and components can be isolated and identified, and (2) the amplitude of each distinct vibration component will remain constant unless there is a change in the operating dynamics of the machine train.

Furthermore, movement generated by vibration can be described mathematically by simple harmonic motion Formulas where position, velocity, and acceleration can be described as a function of time.

Position for a particle under oscillation as a function of time is described by Formula (10) where x position is in reference to its initial position at rest; velocity, and acceleration are Formulas (11,12) respectively.

$$x = A * \cos(wt + \vartheta) \qquad \text{Formula (10)}$$

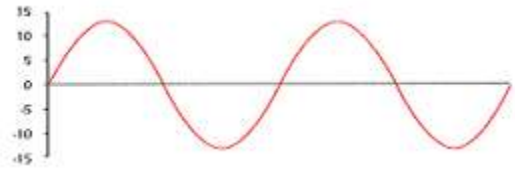

Figure 13 - Particle position as a function of time.

The velocity of the particle is described as $\frac{dx}{dt}$ on Formula (5), and its acceleration as on Formula (6).

$$\dot{x} = -wA * \sin(wt + \vartheta) \qquad \text{Formula (11)}$$

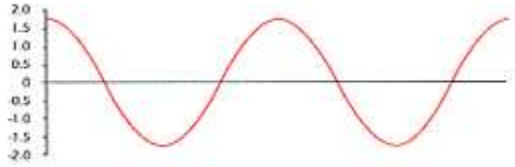

Figure 14 - Particle velocity as a function of time.

$$\ddot{x} = -w^2 A * cos(wt + \vartheta) \qquad \text{Formula (12)}$$

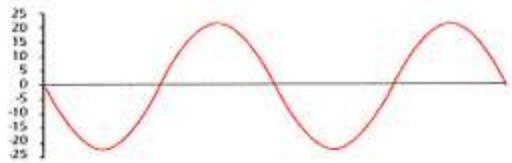

Figure 15 - Particle acceleration as a function of time.

Where
$w =$ angular speed in rad/s
$t =$ time in s
$A =$ constant
$\vartheta =$ phase angle shift

The time it takes for one cycle is called period which is expressed as T and it is inversely proportional to frequency f as expressed on Formula (13); in addition, the relationship between angular velocity w and frequency f is on Formula (14) $w = 2\pi f$ where f is in Hz, and T is in seconds.

$$f = \frac{1}{T}$$ Formula (13)

$$w = 2\pi f$$ Formula (14)

All mechanical systems generate a unique frequency called natural frequency. When a mechanical system is subjected to an external force, it will generate a frequency that depends on mass and stiffness as denoted on Formula (15) where k= stiffness in $\frac{N}{m}$, and m= mass in kg, and f_n in Hz.

$$f_n = \frac{1}{2\pi}\sqrt{\frac{k}{m}}$$ Formula (15)

The ratio between stiffness and mass is directly proportional to the square of the frequency w in $\frac{rad}{s}$ as presented on Formula (16).

$$w^2 = \frac{k}{m}$$ Formula (16)

From Formulas (15-16), k is proportional to the modulus of elasticity, and the Formula implies that the greater the stiffness, the higher the frequency that will be generated; by increasing the mass it will reduced the system frequency or natural frequency. The amplitude of the wavelength depends on the amount of force that is applied on the system.

3.2 Energy Analysis and Fatigue Failure

Mechanical vibration has been monitored on bearing housings to evaluate actual conditions and to predict failure on gears and bearings for a rebar steel plant over a 5 years period. Gears and bearings needed to transmit the necessary energy for rolling billets with physical dimensions of a cross section area of 5.25” x 5.25 “ with a length of between 180” – 220 “ and a mass between 750 kg - 1000 kg that at the end of processing complies with ASTM A615 and ASTM A706 standards. The equipment used for measuring, collecting data, and for analysis was the Emerson CSI 2130 analyzer, the Emerson accelerometer model A0760GP, and AMS Suite: Machinery Health Manager V5.61 software used for a more detailed frequency analysis (Figure 16).

Figure 16 – Emerson CSI 2130 Analyzer and accelerometer A0760GP.

A failure on a gear and a bearing starts on material's surface and it progressively deteriorates with time if no brittle fracture occurs as shown on Figure 17 (a) with none or minimum amount of wear on its surface. However, the unwanted cyclic stresses are acting against material at a continuous rate that will initiate failure on material. This localized initiation failure changes the vibration amplitude of the system, and it will tend to propagate as presented on Figure 17 (b-d).

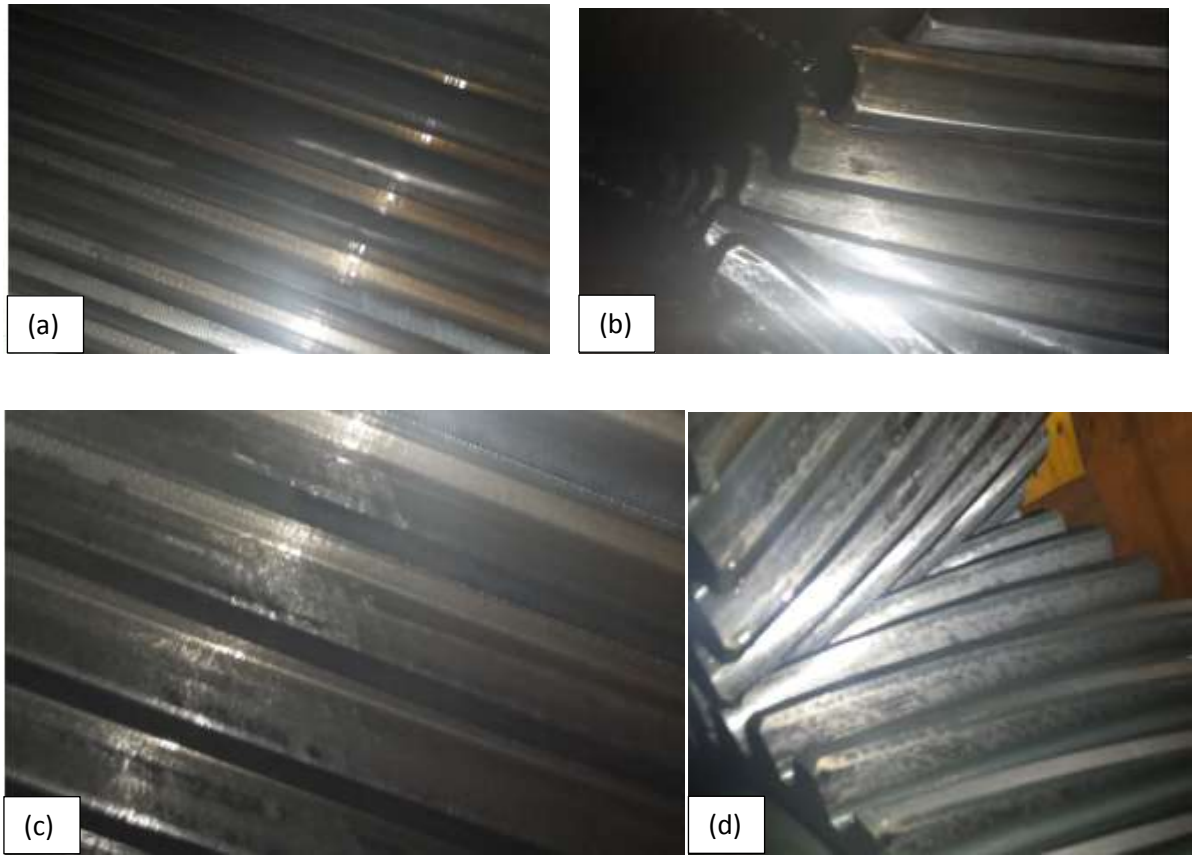

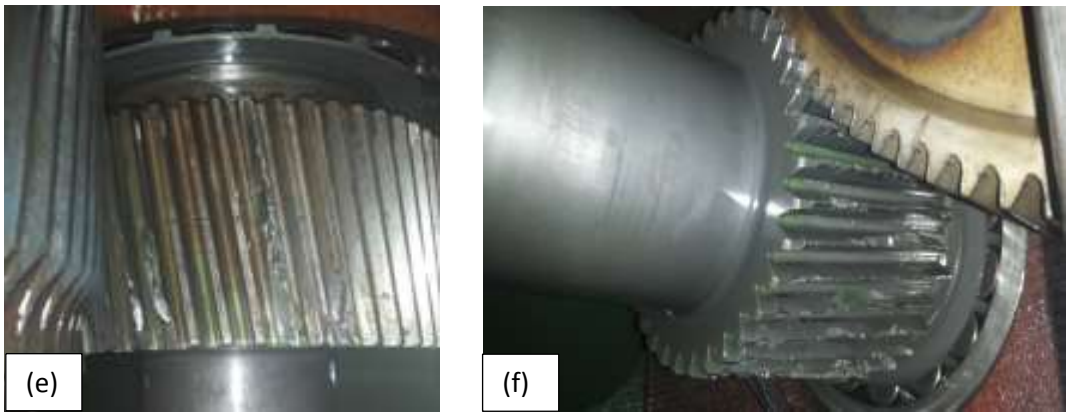

Figure 17 - Materials failure stages of gears. (a) Stage 1 - minimum amount of wear signs on gear surface. (b, c, and d) Stage 2 Pitting and wear at different surface areas (surface failure initiation). (e) and (f) Stage 3 – Fracture and/or deformation of gear's material.

Material failure on gears or bearings starts when they are exposed to mechanical forces that exceed the yield strength on any of their three axes, or because of fatigue failure was caused by cyclic loading. Mechanical vibration or cyclic stresses lead to fatigue failure on mechanical systems; the primary cause of failure is fatigue, the secondary cause is impact, the third cause is wear, and forth is stress rupture. (Metals Handbook, 1978). The most common fatigue stresses are generated by misalignmet, unbalance, and looseness; the characteristic patterns are observed on spectrums respectively as shown on Figure (18).

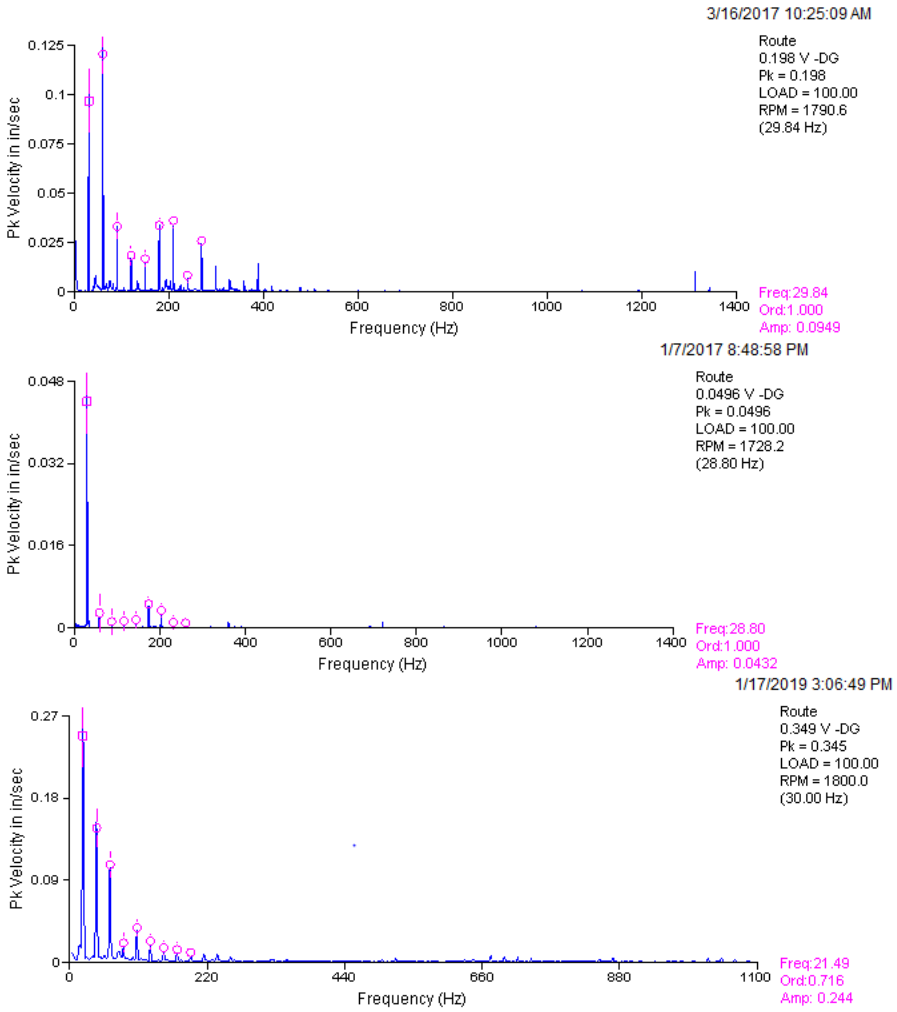

Figure 18 – (a) Misalignment cyclic stress occurring at a frequency of 29.4 Hz. (b) Unbalance cyclic stress generated at a frequency of 28.8 Hz. (c) Looseness pattern frequency at a rate of 30 Hz.

Another important frequency is generated by gears and it is calculated by Formula $GMF = N_T * R_S$ where GMF is gear mesh frequency, N_T is the number of teeth on gear, and R_S is the shaft rotating speed in cycles per second or Hz units. On Figure (19) is the frequency at 243.7 Hz generated by a 37 teeth gear rotating at a speed of 395 rpm (6.583 Hz). The amplitude and sidebands are kept monitored for any change on them to its behavior and tendency in the long term.

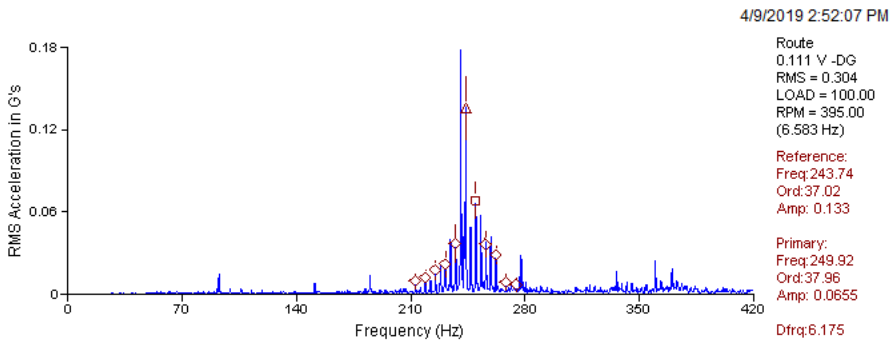

Figure 19 – Gear Mesh Frequency for a 37 teeth gear rotating at a speed of 6.583 rps.

In addition, bearings are critical components in the industry that can cause significant monetary losses if failure occurs, they are designed to withstand high amounts of loads acting in the radial and axial direction. However, if they are exposed to high vibration levels and to inconvenient ambient conditions failure will occur. Therefore, when a defect or imperfection has initiated on a bearing component with the exception of a seal, it generates a unique defect frequency that are detailed in Formulas (17-20).

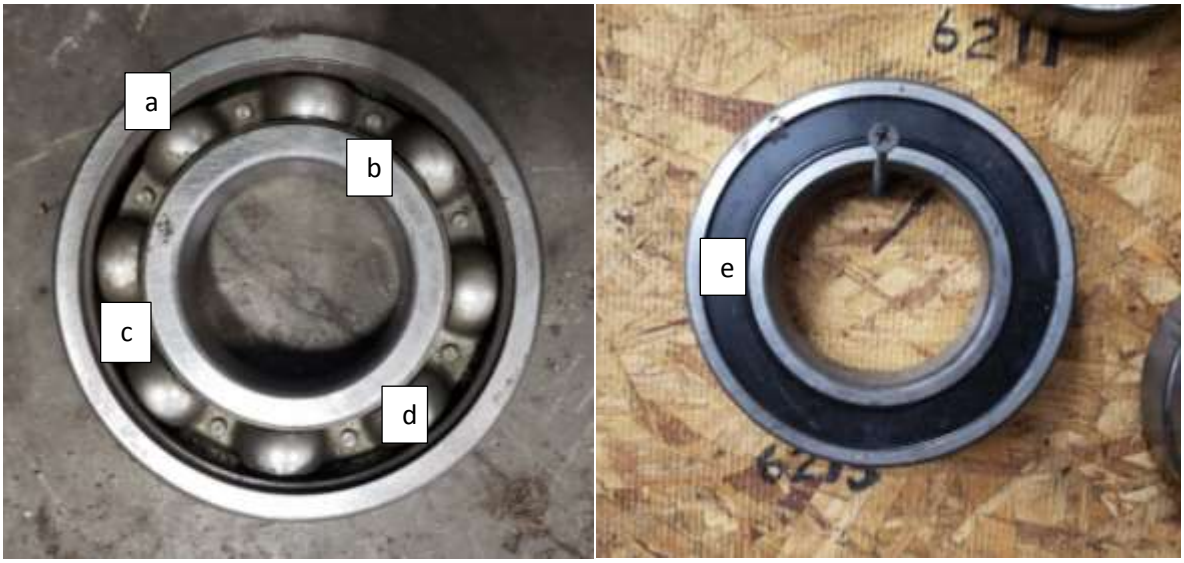

Figure 20 – Bearing components. (a) Outer race. (b) Inner race. (c) Cage. (d) Ball or roller bearing. (e) Bearing seal

$FTF = \frac{S}{2}(1 - \frac{Bd}{Pd}\cos\theta)$	Track/Cage defect frequency	Formula (17)
$BPFI = \frac{Nb*S}{2}(1 + \frac{Bd}{Pd}\cos\theta)$	Inner race defect frequency	Formula (18)
$BPFO = \frac{Nb*S}{2}(1 - \frac{Bd}{Pd}\cos\theta)$	Outer race defect frequency	Formula (19)
$BSF = \frac{Pd*S}{2Bd}(1 - (\frac{Bd}{Pd})^2(cos\theta)^2$	Ball spin defect frequency	Formula (20)

Where,

S =revolutions per second

Bd = Ball or roller diameter

Nb = Number of balls or rollers

Pd = Pitch diameter

θ = Contact angle

The different stages that were described on Figure 17 for how material surface failure tends to initiate and to propagate on gears and bearings, these stages have been correlated to vibration levels based on a 5 years frame. Consequently, Stage I is for normal and stable operating levels; on Stage II the severity is tending to increase and material physical conditions may start to present some defects, it is also the initiation to failure; Stage III are high vibration levels and it has become unstable, subsequently, at any time mechanical failure can occur. Furthermore, the range for Stage I is between 0.03 in/s to 0.06 in/s, Stage II is 0.07 in/s to 0.12 in/s, and lastly on Stage III is higher than 0.13 in/s as presented on Figure (21). Reliability is highly dependent on operating procedures.

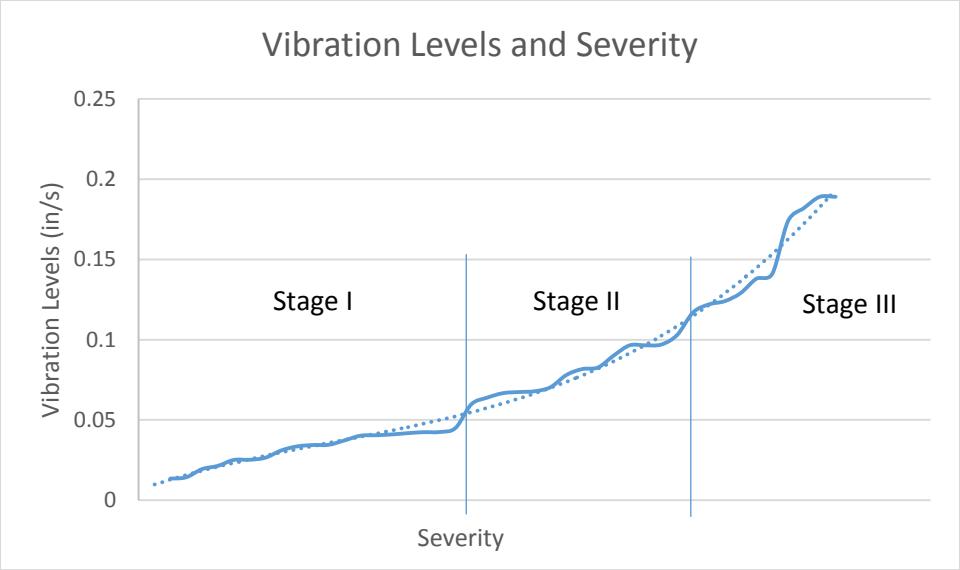

Figure 21 - Vibration levels and severity stages.

The energy loss in the form of mechanical vibration was calculated on Table 7 by using 4 case studies on gearboxes used for rolling milling. These gearboxes are designed to multiply the input torque between 7.2 to 16.52 from a driven force motor of between 600 HP to 1000 HP, and these gearboxes have a mass of between 4000 Kg to 6500 Kg. As a result, the acceleration, velocity, and displacement values were taken from data collected and it has been included on Appendix 1. The total amount of work energy was calculated from Formula (12) where W is work energy in joules (J), F is force in newtons (N), and d is distance in meters (m).

$$W = F * d = m * a * d \qquad \text{Formula (21)}$$

Hence, the displacement of one period was multiplied by the number of revolutions per minute times 60 to obtain the amount of distance traveled by the oscillations generated by vibration on one hour, and this is presented on Table 6. As a result, a mass of 6500 Kg was taken for consideration and multiplied by the respective acceleration from spectrums and waveforms obtained from software analysis on Appendix 1. The total amount of energy per hour, per day, and per 6 months period was obtained on Table (7).

Table 5 – Total displacement calculation in one hour for values obtained from Appendix 1.

		Velocity		Displacement		
		in/s	m/s	Mils per cycle	Meters per cycle	Total displacement in one hour (m)
Gearbox 1						
Before	Horizontal	0.1300	0.00330200	18.600	0.000472440	9.581083
3/26/2015	Vertical	0.0594	0.00150880	5.643	0.000143332	2.906777
338 rpm	Axial	0.1820	0.00462280	25.650	0.000651510	13.212623
After	Horizontal	0.0592	0.00150368	10.230	0.000259842	2.962199
7/25/2015	Vertical	0.0156	0.00039624	5.893	0.000149682	1.706377
190 rpm	Axial	0.0434	0.00110236	135.360	0.003438144	39.194842
Gearbox 3						
Before	Horizontal	0.2380	0.00604520	41.560	0.001055624	22.358116
2/16/2015	Vertical	0.2210	0.00561340	2.530	0.000064262	1.361069
353 rpm	Axial	0.1380	0.00350520	18.650	0.000473710	10.033178
After	Horizontal	0.0437	0.00111000	13.470	0.000342138	6.815389
6/22/2015	Vertical	0.0179	0.00045470	9.985	0.000253619	5.052090
332 rpm	Axial	0.0230	0.00058420	4.697	0.000119304	2.376532
Gearbox 4						
Before	Horizontal	0.1540	0.00391160	13.430	0.000341122	8.739546
8/15/2017	Axial	0.3670	0.00932180	17.610	0.000447294	11.459672
427 rpm						
After	Horizontal	0.0340	0.00086360	6.084	0.000154534	4.218767
9/12/2017	Axial	0.0414	0.00105156	9.365	0.000237871	6.493878
455 rpm						
Gearbox 5						
Before	Horizontal	0.1750	0.00444500	62.400	0.001584960	35.566502
4/10/2017	Axial	0.2030	0.00515620	39.740	0.001009396	22.650846
374 rpm						
After	Horizontal	0.0360	0.00091440	16.860	0.000428244	9.712574
7/16/2017	Axial	0.0408	0.00103632	11.710	0.000297434	6.745803
378 rpm						

Table 6 – Mechanical vibration energy and percent difference.

		Acceleration		Energy in Joules			
		G's	m/s^2	1 hour	1 month	6 months	
Gearbox 1							
Before	Horizontal	0.14	1.3720	2,079,052	62,371,564	374,229,384	
3/26/2015	Vertical	0.0607	0.5949	273,478	8,204,354	49,226,124	
338 rpm	Axial	0.198	1.9404	4,054,870	121,646,107	729,876,640	
							% difference
After	Horizontal	0.0638	0.6252	292,926	8,787,774	52,726,643	-86
7/25/2015	Vertical	0.00968	0.0949	25,602	768,059	4,608,352	-91
190 rpm	Axial	0.0459	0.4498	2,788,459	83,653,783	501,922,699	-31
Gearbox 3							
Before	Horizontal	0.408	3.9984	14,138,981	424,169,426	2,545,016,554	
2/16/2015	Vertical	0.191	1.8718	402,936	12,088,086	72,528,517	
353 rpm	Axial	0.138	1.3524	2,146,052	64,381,573	386,289,436	
							% difference
After	Horizontal	0.0569	0.5576	601,071	18,032,125	108,192,748	-96
6/22/2015	Vertical	0.0157	0.1539	122,940	3,688,203	22,129,215	-69
332 rpm	Axial	0.0256	0.2509	94,299	2,828,965	16,973,790	-96
Gearbox 4							
Before	Horizontal	0.044	0.4312	596,025	17,880,741	107,284,447	
8/15/2017	Axial	0.0624	0.6115	1,108,357	33,250,699	199,504,192	
427 rpm							
							% difference
After	Horizontal	0.0238	0.2332	155,627	4,668,813	28,012,880	-74
9/12/2017	Axial	0.0351	0.3440	353,292	10,598,765	63,592,588	-68
455 rpm							
Gearbox 5							
Before	Horizontal	0.0419	0.4106	2,309,819	69,294,564	415,767,386	
4/10/2017	Axial	0.0513	0.5027	1,801,045	54,031,346	324,188,074	
374 rpm							
							% difference
After	Horizontal	0.0168	0.1646	252,910	7,587,306	45,523,837	-89
7/16/2017	Axial	0.0201	0.1970	210,161	6,304,835	37,829,008	-88
378 rpm							

Table 7 – Number of cycles with given rpm.

Number of Cycles				
rpm	Cycles per 1 hour	Cycles per 1 day	Cycles per 3 months	Cycles per 6 months
338	20280	486720	43.8E+06	8.8E+07
358	21480	515520	46.4E+06	9.3E+07
427	25620	614880	55.3E+06	1.1E+08
455	27300	655200	59.0E+06	1.2E+08

Therefore, the total number of cycles at which equipment was exposed to high mechanical vibration levels and considered in this thesis as being on Stage III has been calculated on Table 8. The number of cycles generated by the turning speed of driven force was calculated on a 3 months and a 6 months period. Hence, under the assigned rpm on input gearboxes they all reached at least 43.8E+06 and 8.8E+07 cycles on 3 months period and 6 months period respectively. Mechanical vibration has a significant impact on gears and bearings reliability used within the steel industry for hot rolling of rebar. It affects the efficiency drastically in the case when they fail during production. The highest impact occurs on reheating processing due to the energy consumption to maintain billets at a temperature of at least of 960°C. Stefan-Boltzmann Formula for radiation energy transmitted is on Formula (22) where P is power in watts (W), σ is Boltzmann constant of $5.67X10^{-8}\frac{W}{m^2*T^4}$, e stands for material emissivity, A is material surface area in m^2. Hence, if e of 0.90 for steel is taken for consideration with a billet surface area of $4.01m^2$ as presented on Formula (23) a total power of 564,030 W is needed.

$$P = \sigma Ae(T^4) \qquad \text{Formula (22)}$$

$$P = \sigma Ae(T^4) = 5.67X10^{-8}\frac{W}{m^2*T^4} * (4.01m^2) * [1255°K]^4 = 564{,}030\ W \qquad \text{Formula (23)}$$

Thus, for every hour of reheating processing it is needed an amount of 2,030.5 MJ to maintain a billet at a temperature of 960°C.

$$P = 564{,}030\ W * 3600s = 564{,}030\ \frac{J}{s} * 3600\ s = 2{,}030{,}508{,}000\ J = 2{,}030.5\ MJ \qquad \text{Formula (24)}$$

In the four cases of study it was concluded that there is a significant percent difference on mechanical vibration energy between before and after the replacement of new or better set of gears and bearings. In 3 out of 4 cases existed a reduction of between 68 percent to 96 percent and on 1 case the reduction was between 31 to 91 percent in terms of energy generated by the movement, or displacement by vibration in relationship to a reference point. Therefore, the materials selected for gears under the American Gear Manufacturers Association (AGMA) satisfied the design criteria by failing progressively.

CONCLUSION

In conclusion, the melting and reheating of steel are the two highest energy consumers within the steel industry. It is needed at least an amount of 2,083.7 MJ for melting, solidification, and reheating a metric ton (MT) of steel. In contrast, it is needed 2030.5 MJ when failure occurs on any mechanical component to maintain billet at the proper temperature for hot rolling for every hour on down time. Based on mechanical vibration analysis and tendencies as a measurement for fatigue, gears and bearings tended to fail progressively by the increase of vibration levels over time. There exist a high potential to reduce energy and material costs if it is applied properly and the most importance and objective for this thesis is that there will be a reduction on greenhouse gas emissions if this system is applied worldwide on steel industries.

REFERENCES

Bordonaro, G. G., Leardi, R., Diviani, L., & Berto, F. (2018). Design of Experiment as a powerful tool when applying Finite Element Method: A case study on prediction of hot rolling process parameters. *Frattura Ed Integrità Strutturale,12*(44), 1-15. doi:10.3221/igf-esis.44.01

Bralla, J. G. (1999). Gears. In Design for Manufacturability Handbook (2nd ed.). McGraw Hill.

Çiftçi, B. (2017). Potential game changers for the future of steel making.

Dudley, D. W., & Townsend, D. P. (1992). Dudleys gear handbook. New York: McGraw-Hill.

Jha, A. R. (2015). Energy technology 2015 Carbon dioxide management and other technologies. Cham: Springer international publishing. Retrieved from https://ebookcentral.proquest.com/lib/utep/detail.action?docID=1979983.

Jyri Outinen, J., & Mäkeläinen, P. (2004). Mechanical properties of structural steel at elevated temperatures and after cooling down. doi.org/10.1002/fam.849.

Karassik, I. J., Messina, J. P., Cooper, P., & Heald, C. C. (2008). Chapter 9 - Speed Varying Devices. In Pump Handbook (4th ed.). McGraw Hill. Retrieved from Access Engineering.

Kiameh, P. (2003). Electrical equipment handbook: Troubleshooting and maintenance. New York: McGraw-Hill.

Mandal, S. K. (2015). Steel metallurgy: Properties, specifications and applications.

Munther, P., & Roberts, W. L. (2008). Chapter 8. Reheat Furnaces. In Hot rolling of steel. New York: CRC.

Rojas Cardenas, J. C., Hasenbeigi, A., Sheinbaum, C., & Price, L. (2017). Energy efficiency in the Mexican iron and steel industry from an international perspective (Abstract).

Sadegh, A. M., Ph.D., & Worek, W. M., Ph.D. (2018). Chapter. Gearing. In Marks' Standard Handbook for Mechanical Engineers, 12th Edition (12th ed.). McGraw-Hill Professional. Retrieved from Access Engineering.

Sahoo, M., & Sahu, S. (2014). Principles of metal casting. New York, NY: McGraw-Hill Education.

Tide, R. H. R. (2003). Integrity of Structural Steel After Exposure to Fire. Retrieved 2003.

Whitaker, J., & Benson, B. (2001). Standard Handbook of Audio Engineering (2nd ed.).

Wu, Y., Su, J., Li, K., & Sun, C. (2019). Comparative study on power efficiency of Chinas provincial steel industry and its influencing factors. *Energy,175*, 1009-1020. doi:10.1016/j.energy.2019.03.144

Zaretsky, E. V., & Branzai, E. V. (2016). Rolling Bearing Service Life Based on Probable Cause for Removal—A Tutorial. Tribology Transactions, 60(2), 300-312. doi:10.1080/10402004.2016.1163761

Zaretsky, E. V., Parker, R. J., & Anderson, W. J. (1967). Component hardness differences and their effect on bearing fatigue. Lubrication Technology, 89(1). doi:10.1016/0043-1648(67)90328-6

APPENDICES

Appendix A – Gearbox 1 Case of Study.
Before replacement. Horizontal mechanical vibration readings. Worn out conditions.

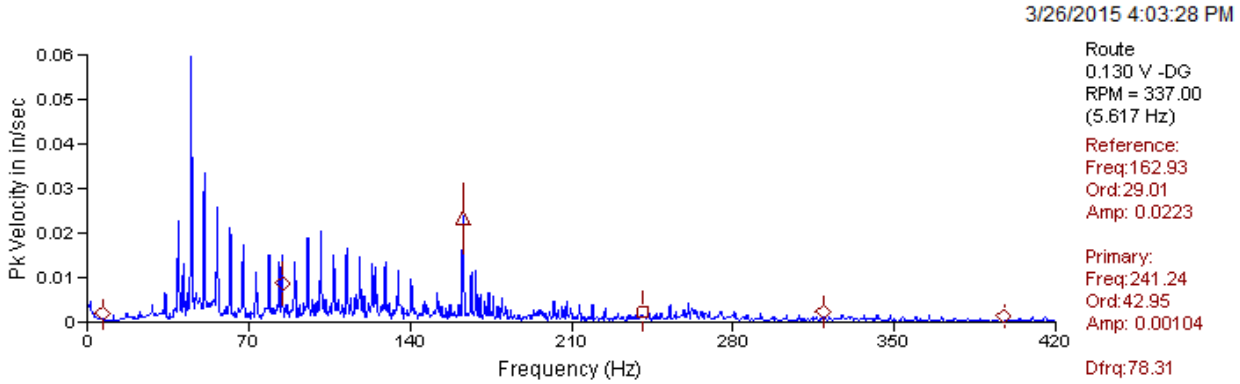

Displacement

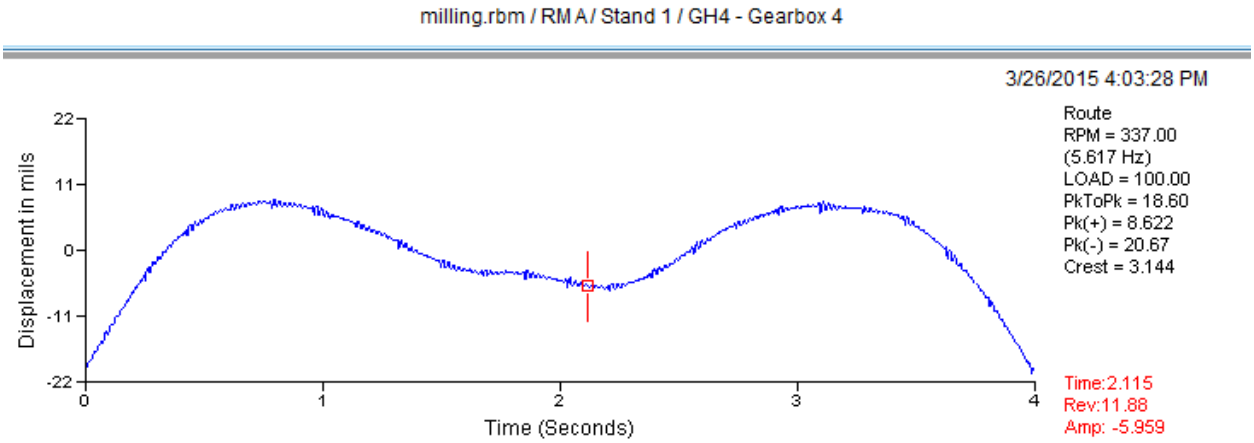

Broken tooth gear pattern.

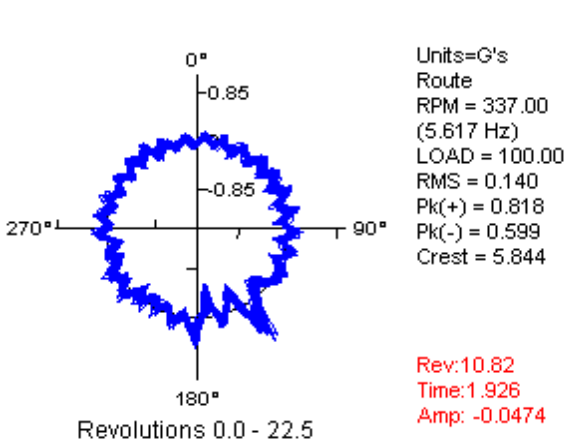

Before replacement. Vertical mechanical vibration readings.
Vertical waveform acceleration. Impacting pattern.

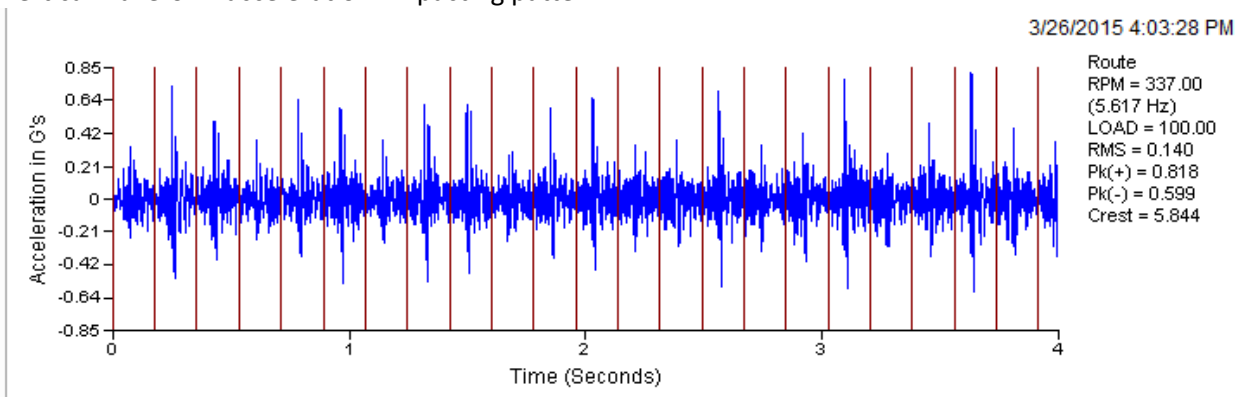

Displacement

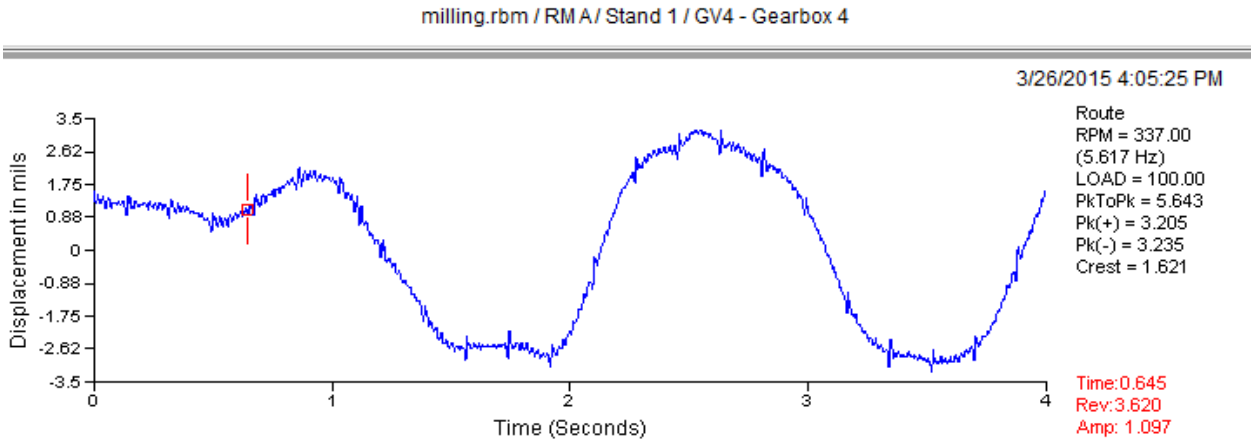

Velocity

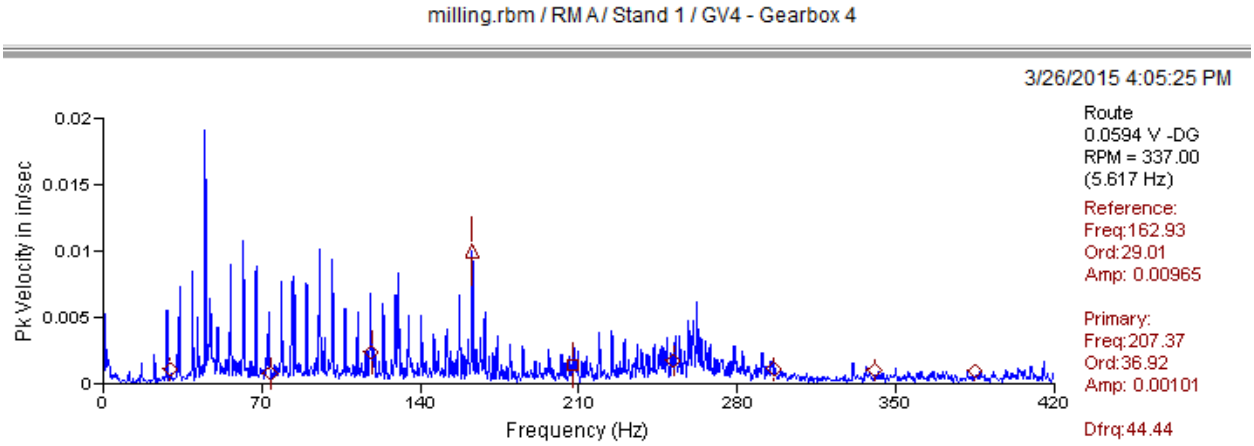

Before replacement. Axial mechanical vibration readings.
Velocity – worn out conditions and wear on spectrum below.

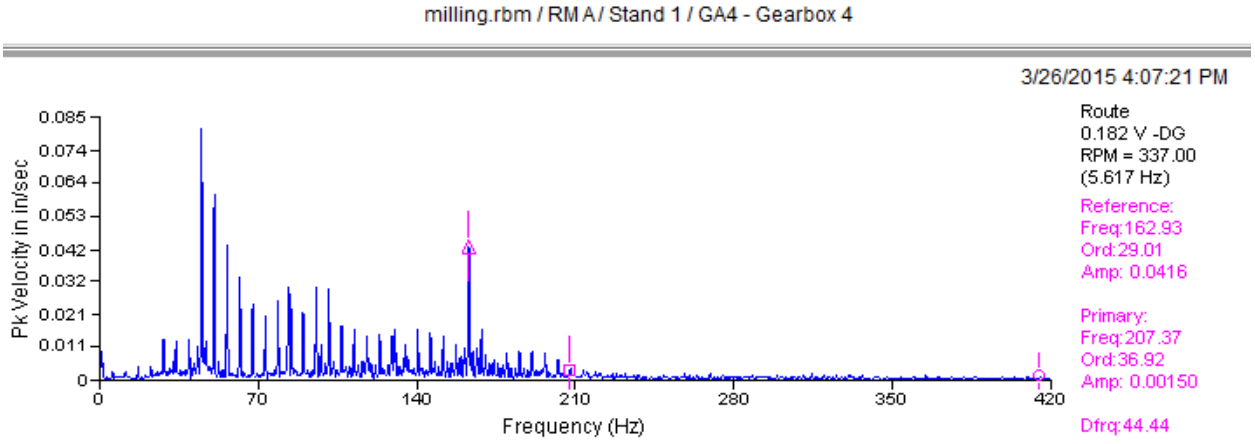

Acceleration – Broken tooth gear pattern.

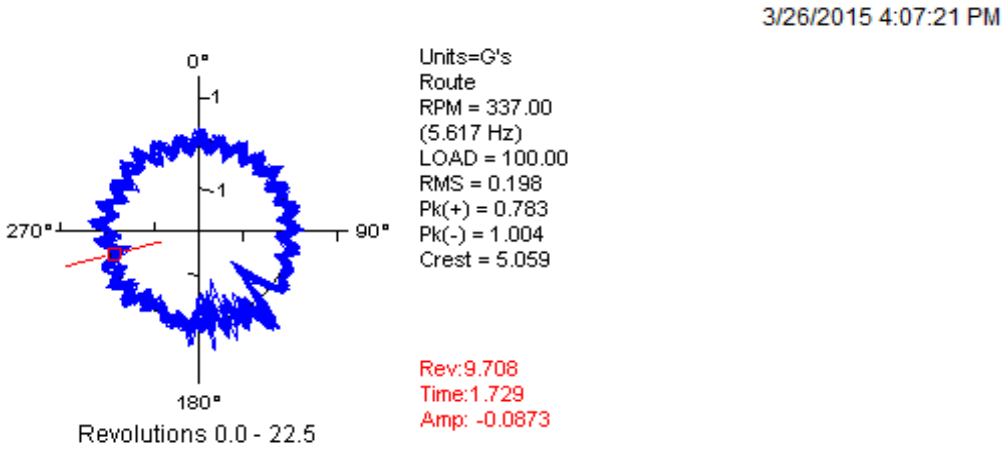

Displacement

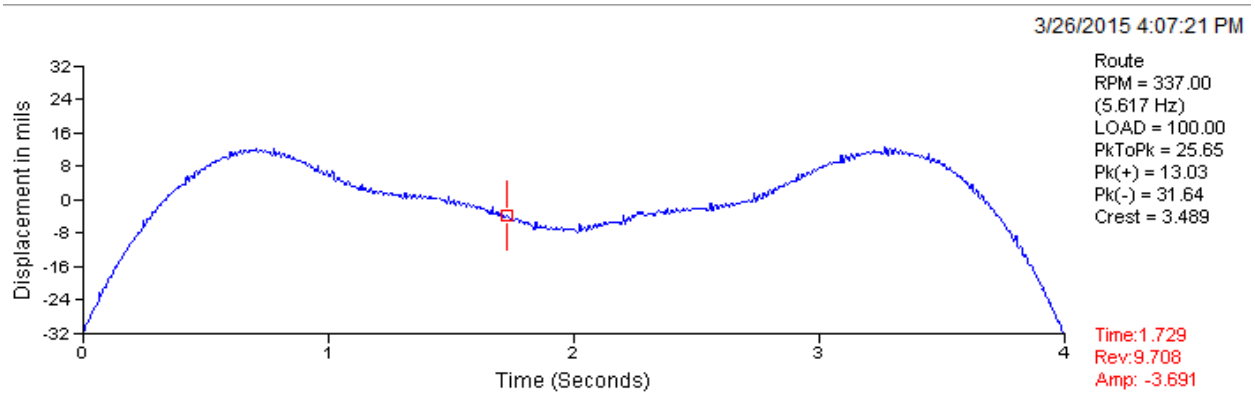

After replacement.
Horizontal mechanical vibration readings.
Velocity.

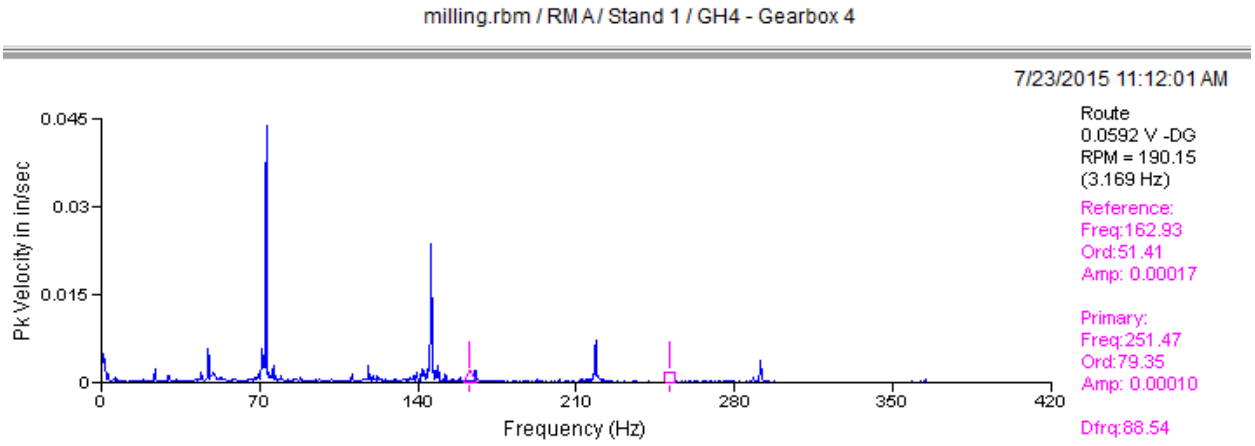

Acceleration

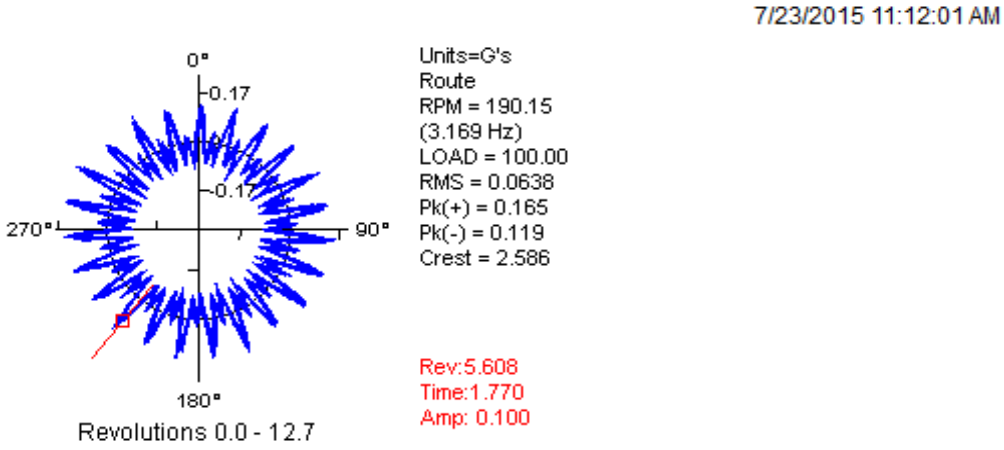

Displacement

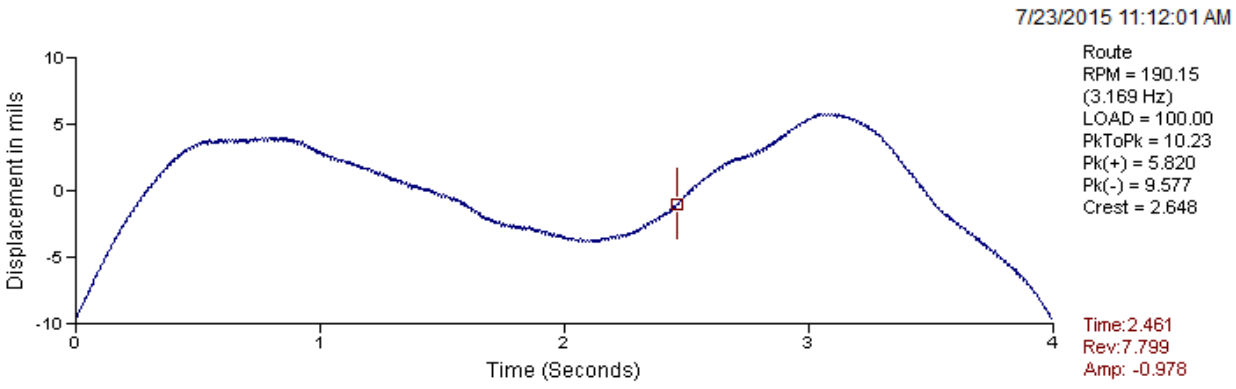

After replacement.
Vertical mechanical vibration readings.
Velocity

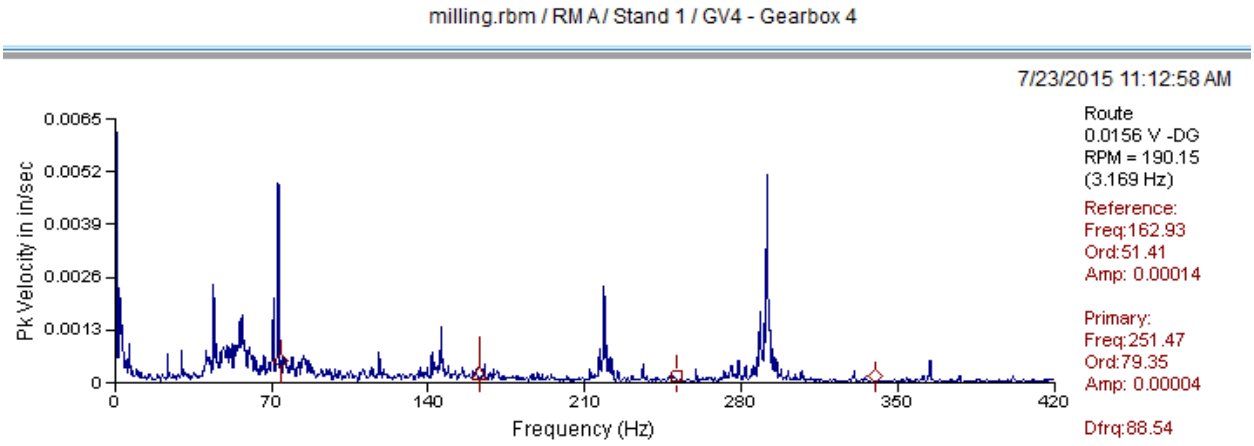

Acceleration – A better stress distribution is observed on waveform below.

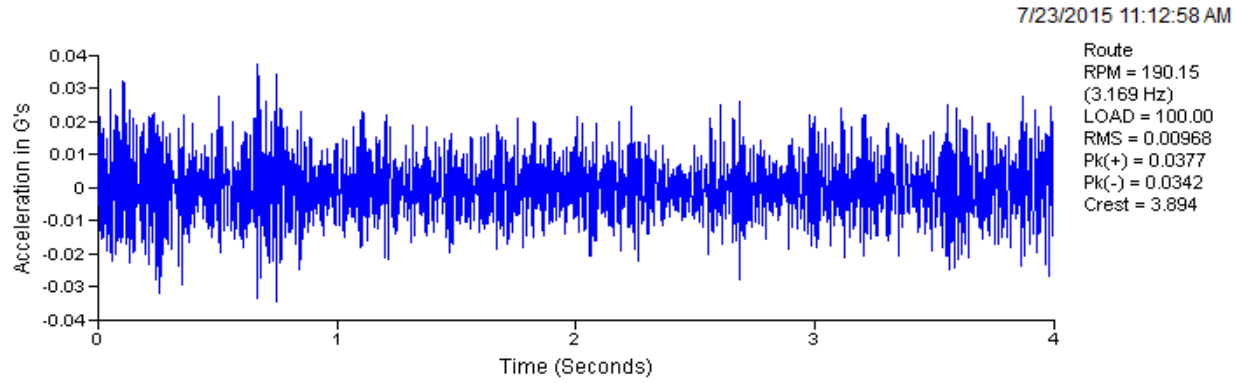

Displacement

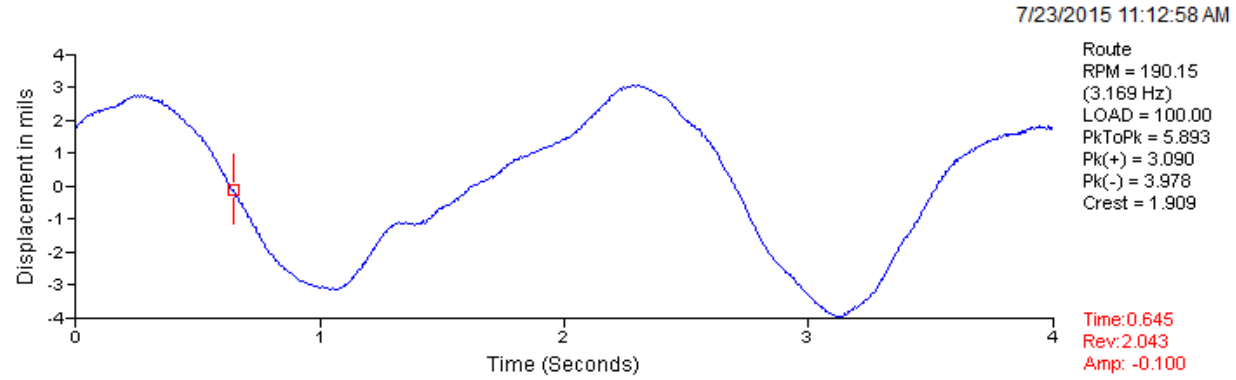

After replacement.
Axial mechanical vibration readings. Velocity, acceleration, and displacement are respectively below.

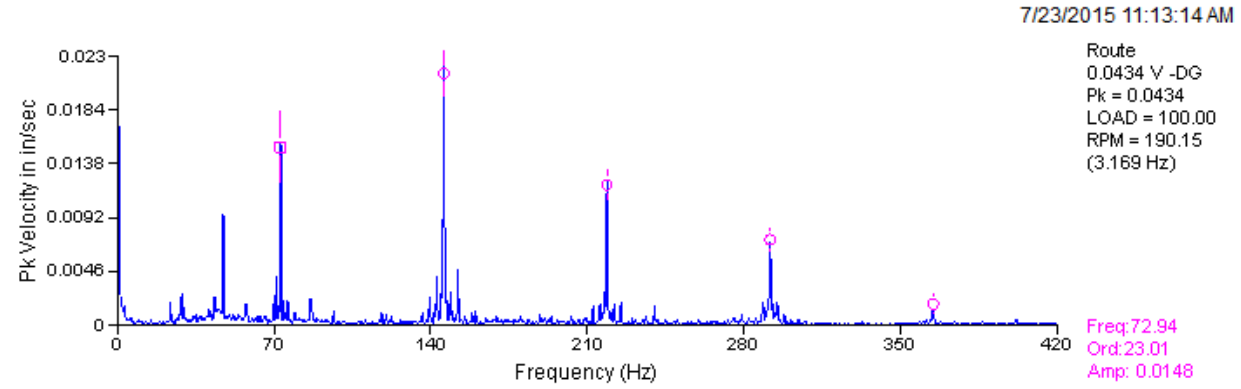

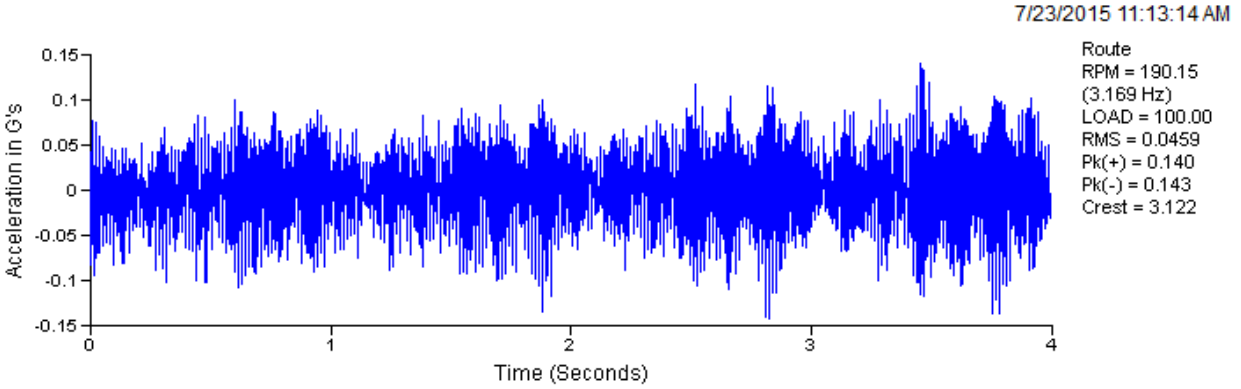

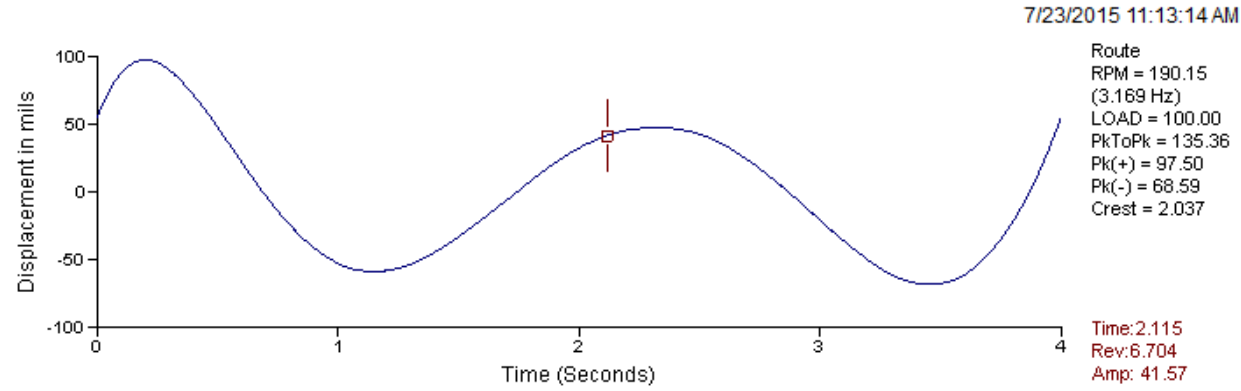

Appendix B – Gearbox 3 Case of Study.

Before replacement readings.

Horizontal vibration readings. Velocity, acceleration, and displacement are respectively below.

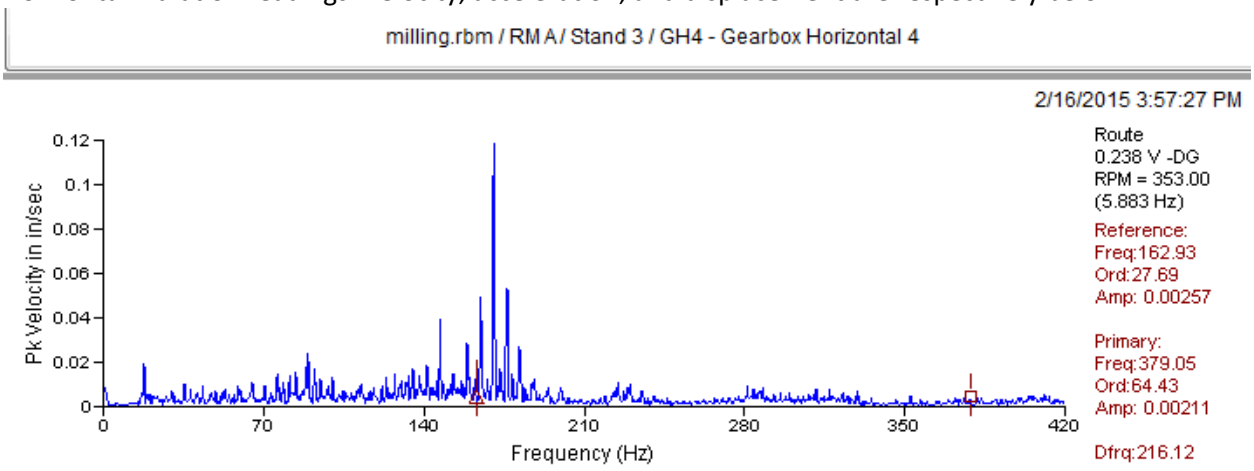

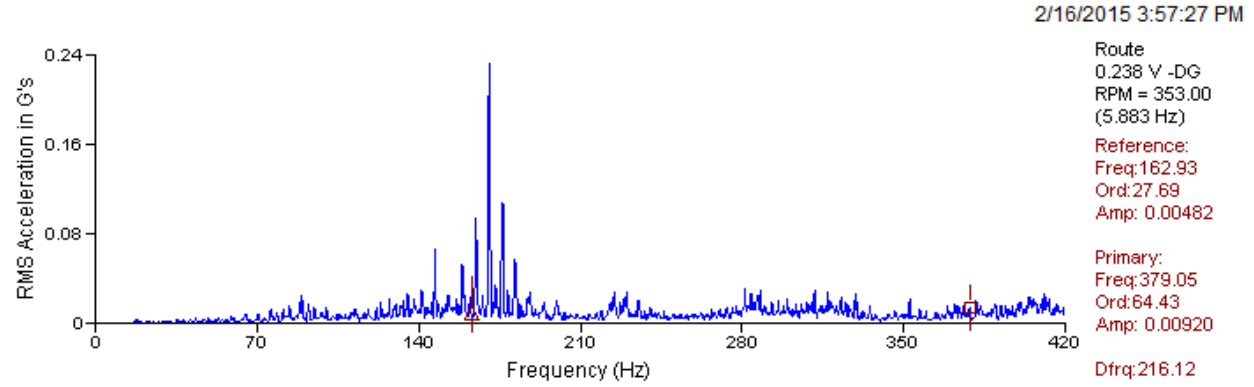

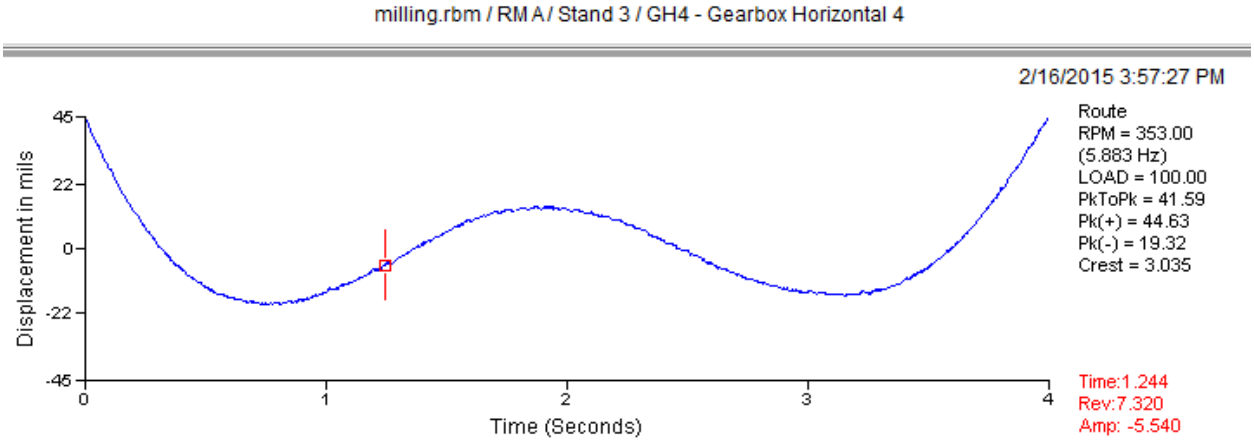

Before replacement readings.
Vertical vibration readings. Velocity, acceleration, and displacement are rspectively below. Worn out patterns.

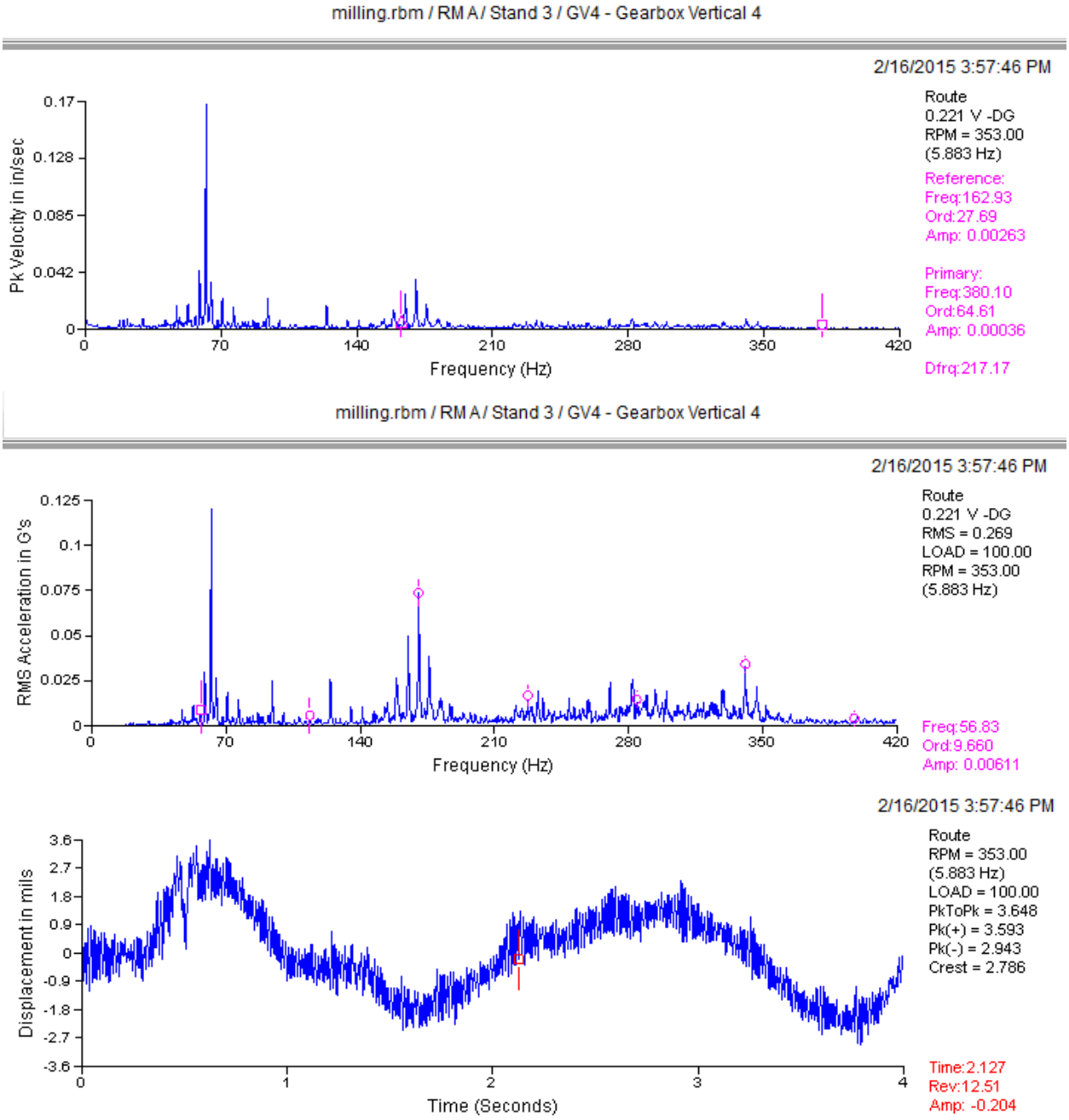

Before replacement readings.
Axial vibration readings. Velocity, acceleration, and displacement are respectively below. Impacting behavior is observed on acceleration.

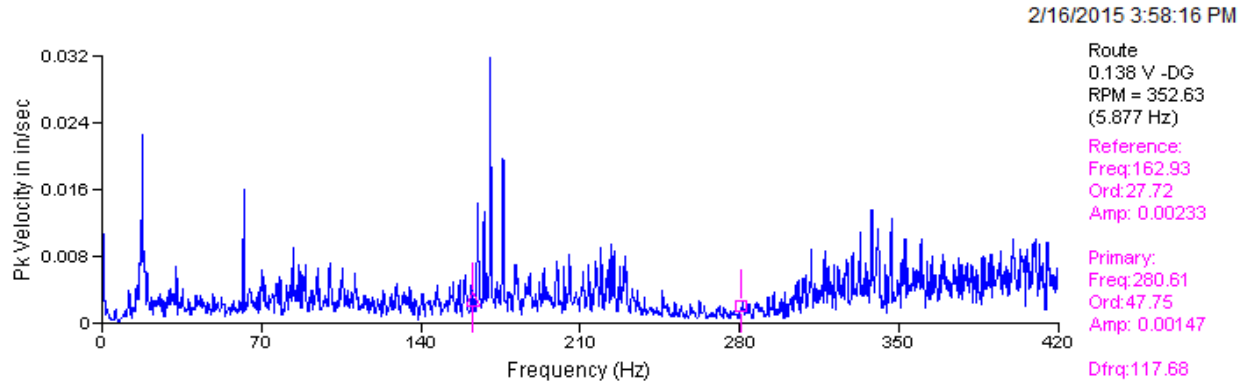

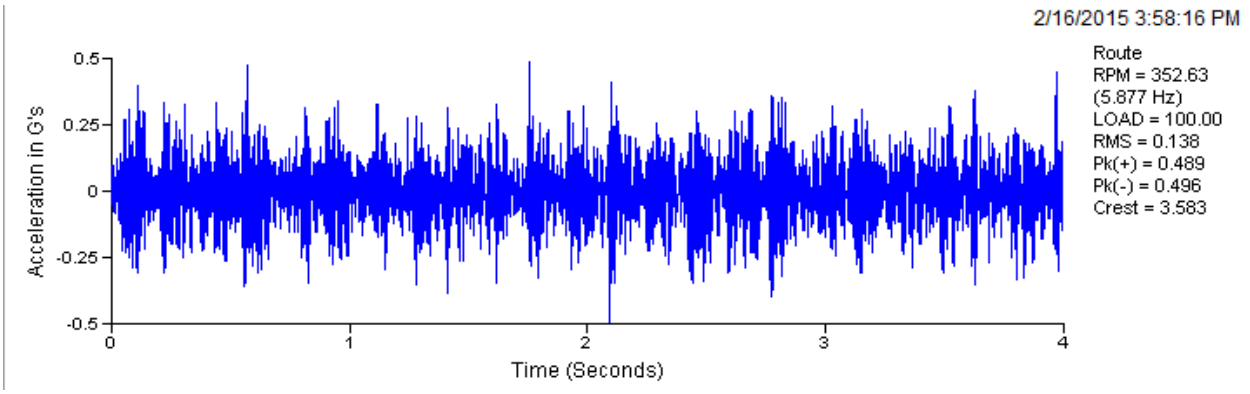

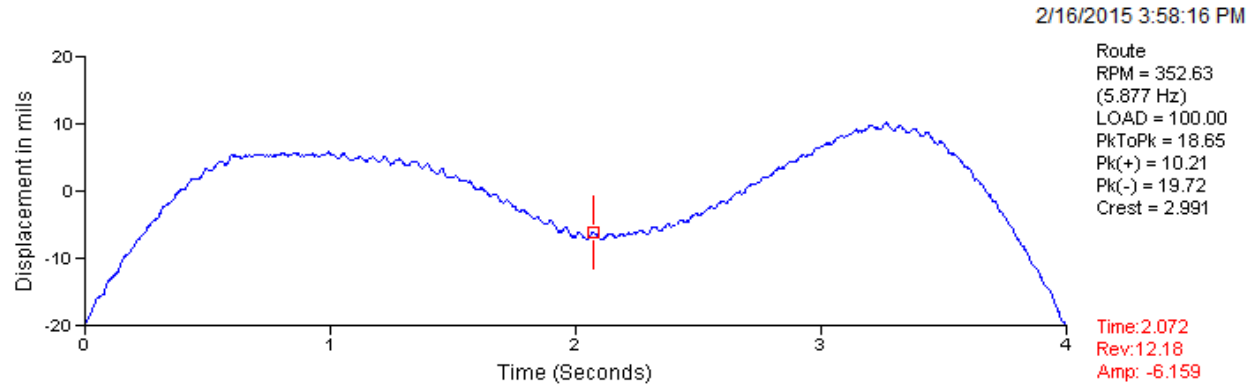

After replacement readings.
Horizontal vibration readings.
Gear mesh frequency below with no side bands meaning conditions are good.

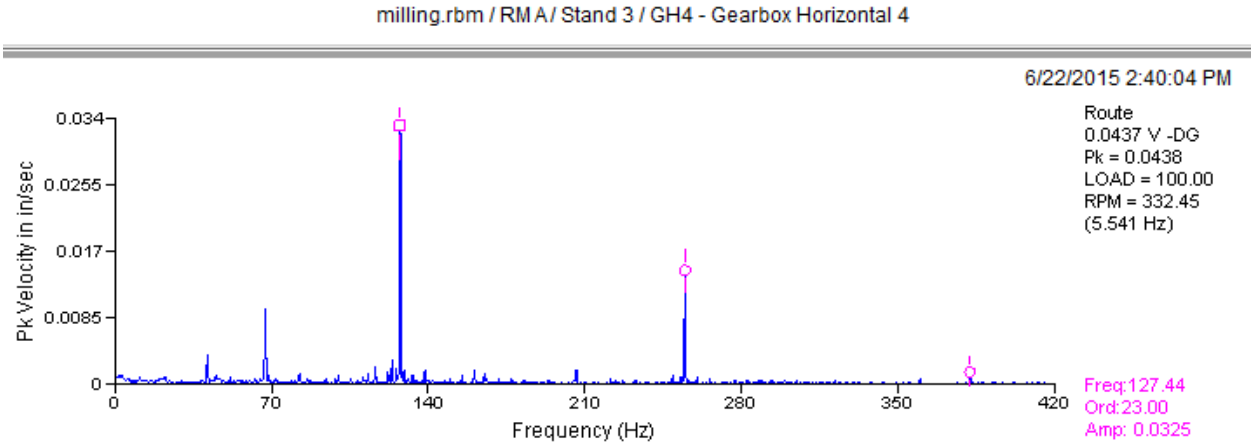

Acceleration

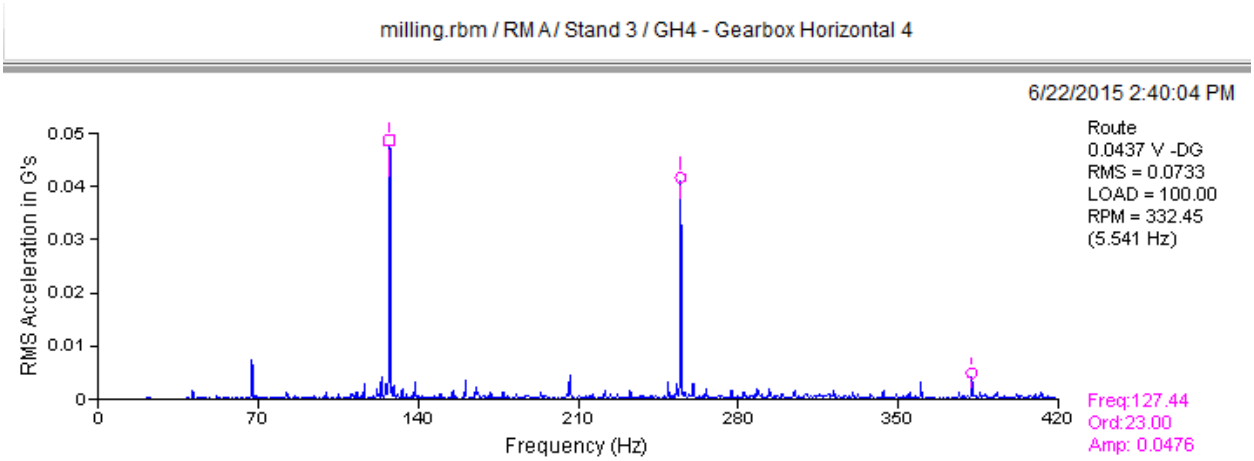

Displacement

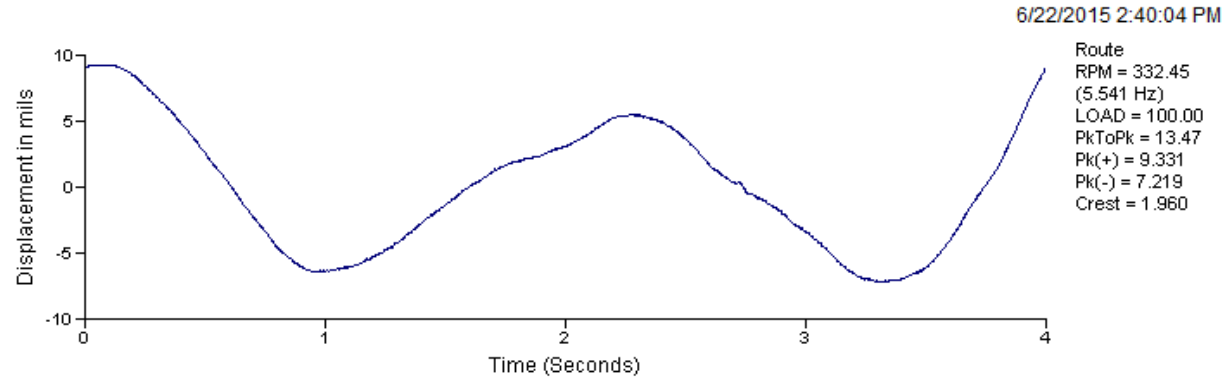

After replacement readings.
Vertical vibration readings. Velocity, acceleration, and displacement are respectively below.

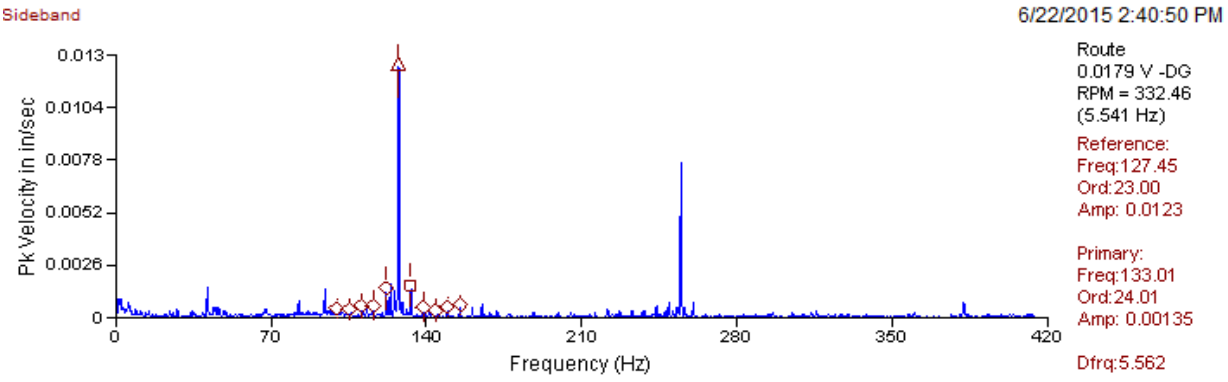

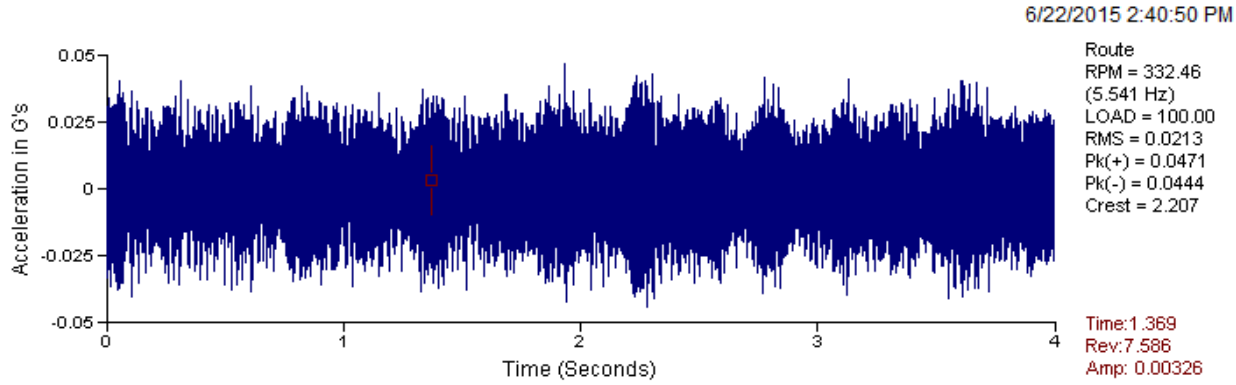

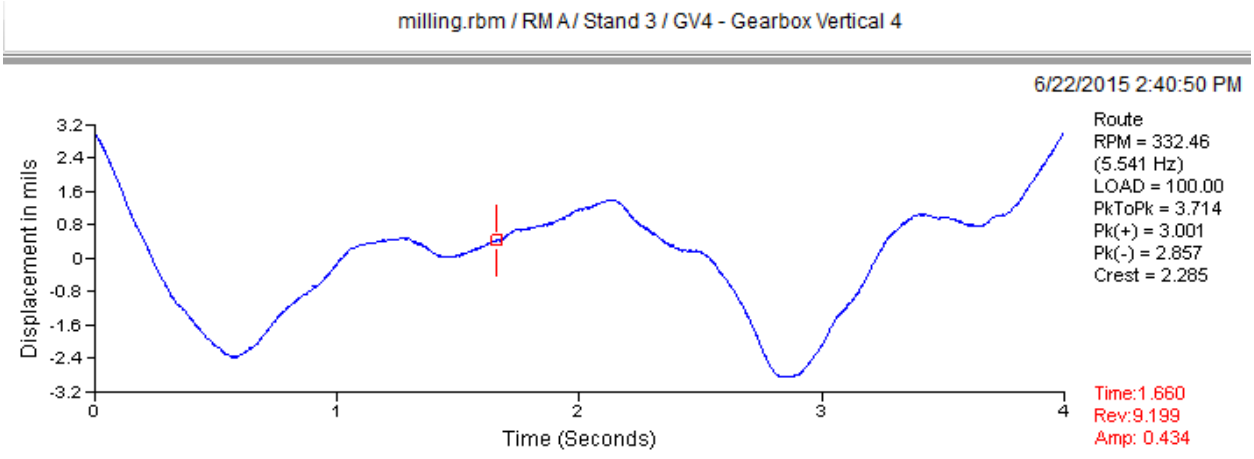

After replacement readings.
Axial vibration readings. Velocity, acceleration, and displacement are respectively below. No more impacting is presented on acceleration waveform as it was before.

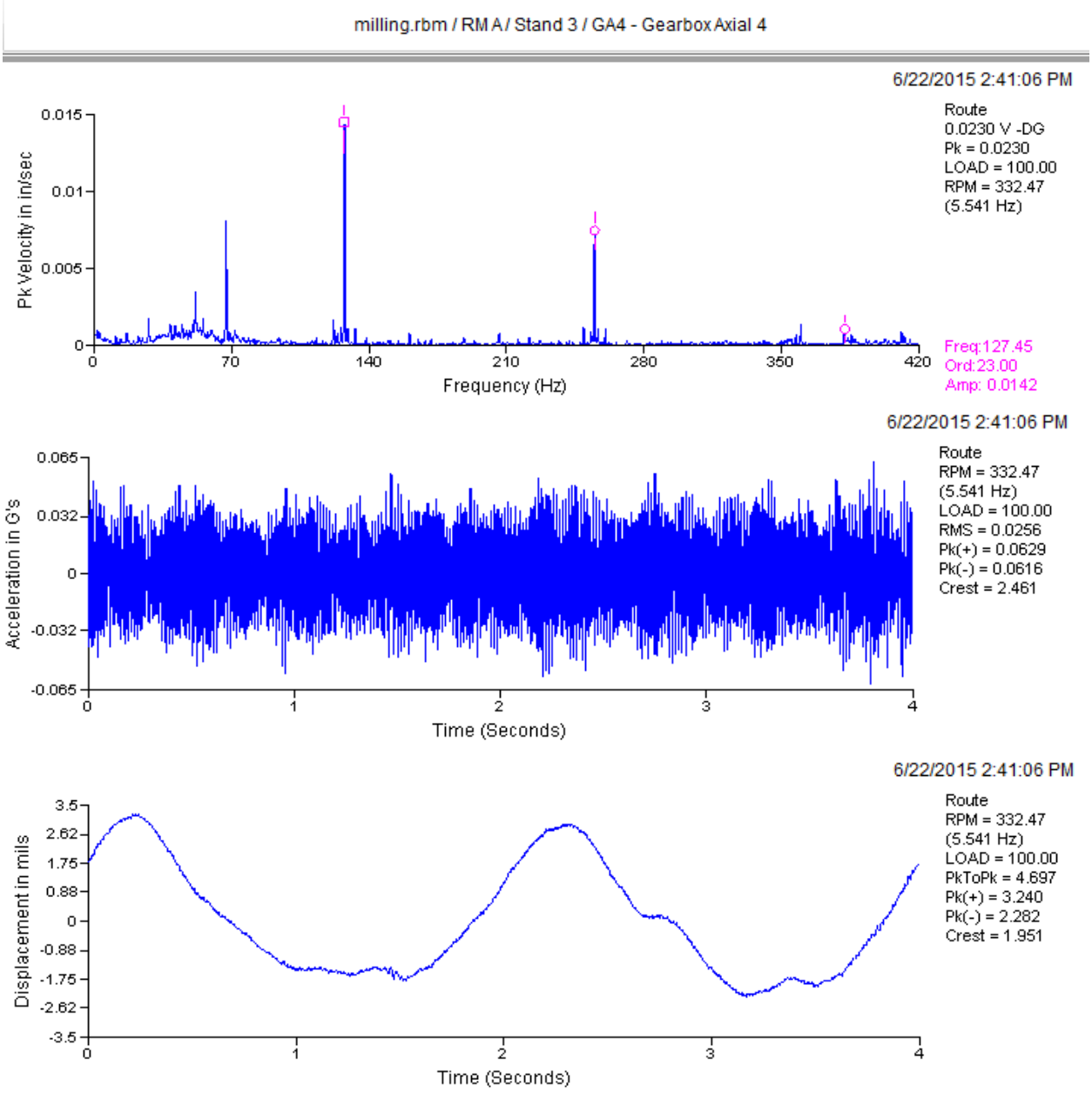

Appendix C– Gearbox 4 Case of Study.
Before replacement readings.
Horizontal vibration readings. Looseness pattern on velocity spectrum below.

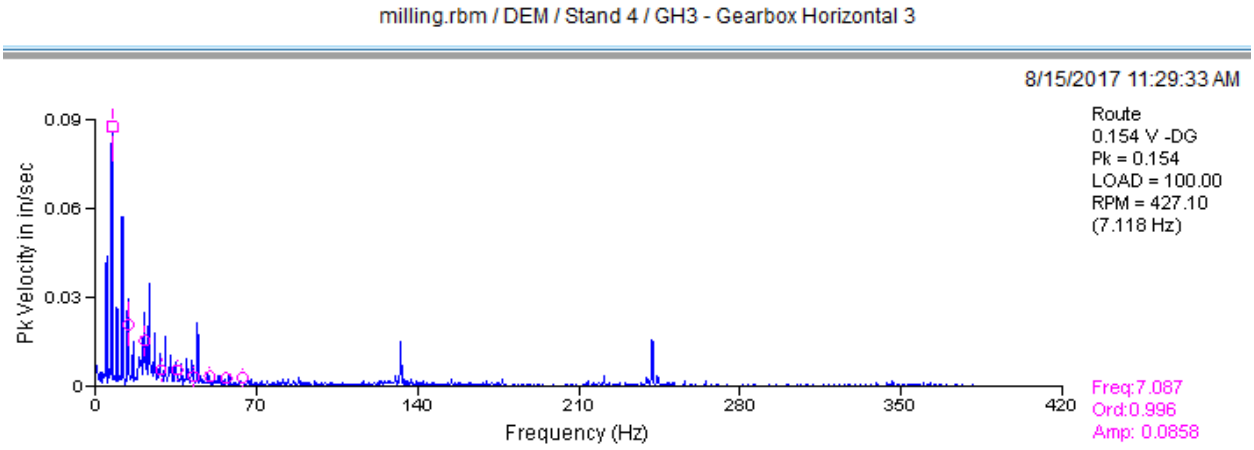

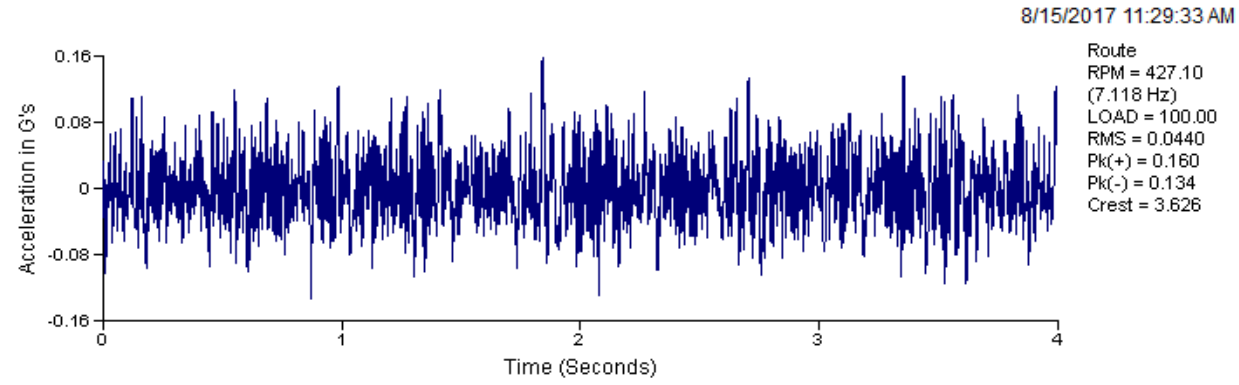

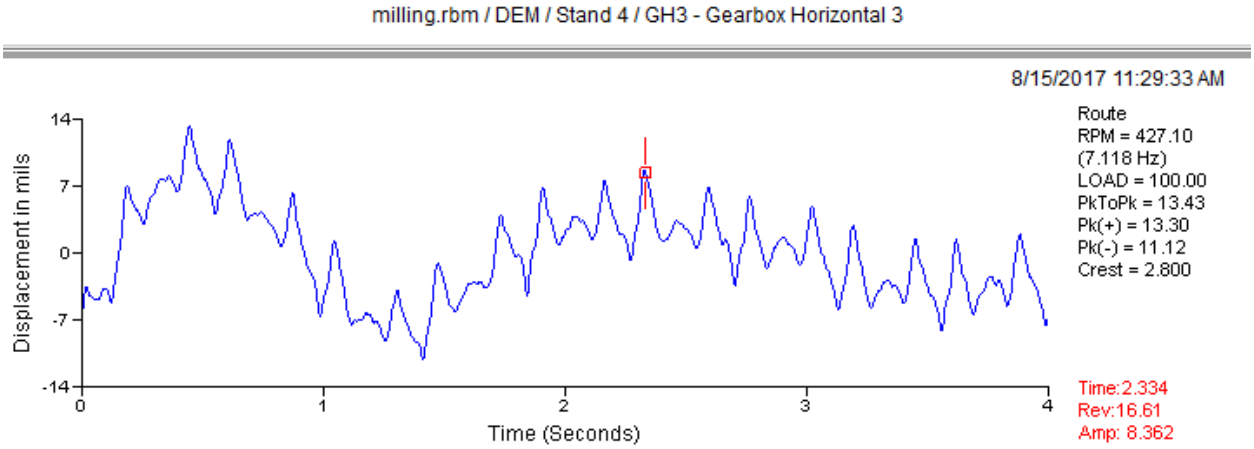

Before replacement readings.
Axial vibration readings.

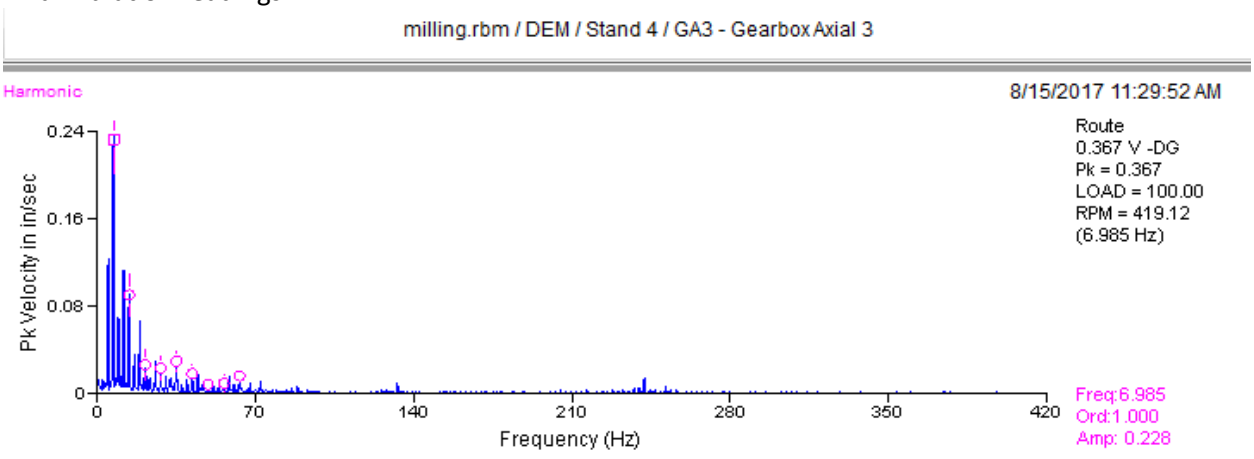

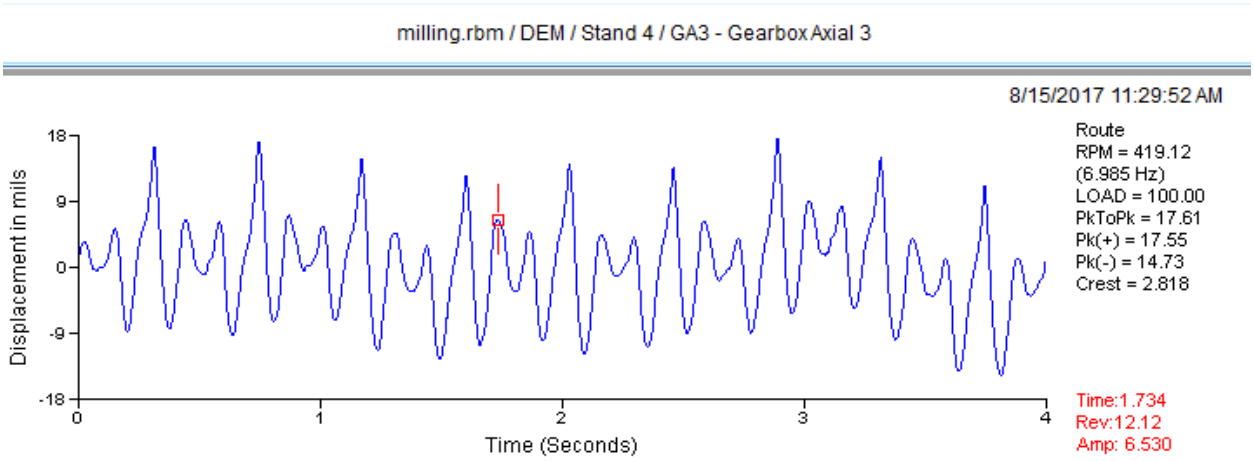

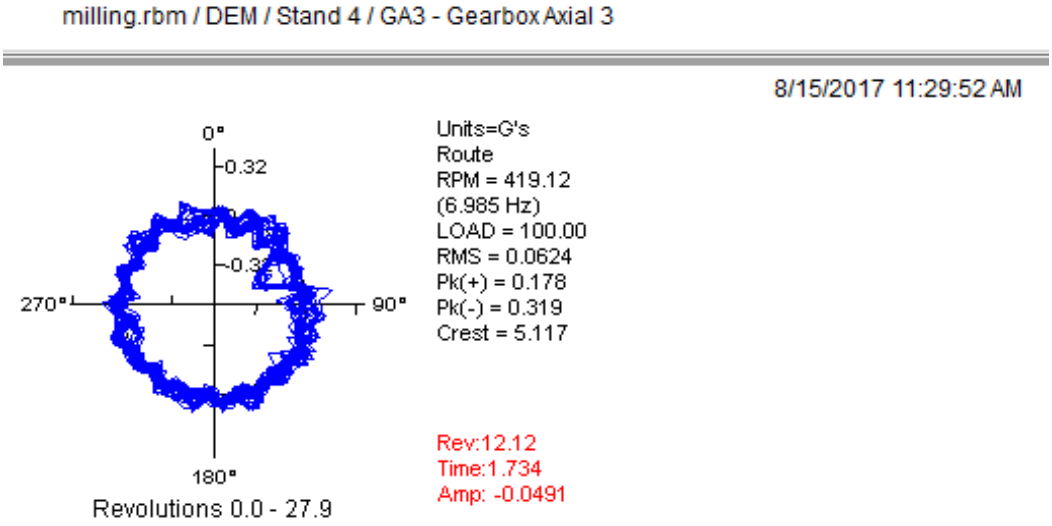

After replacement readings.
Horizontal vibration readings. Velocity, acceleration, and displacement at lower levels than before.

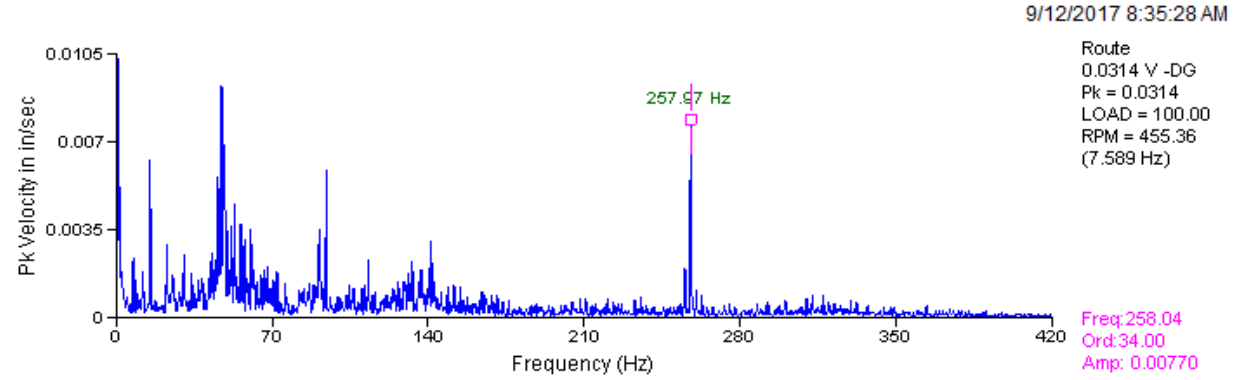

milling.rbm / DEM / Stand 4 / GH3 - Gearbox Horizontal 3

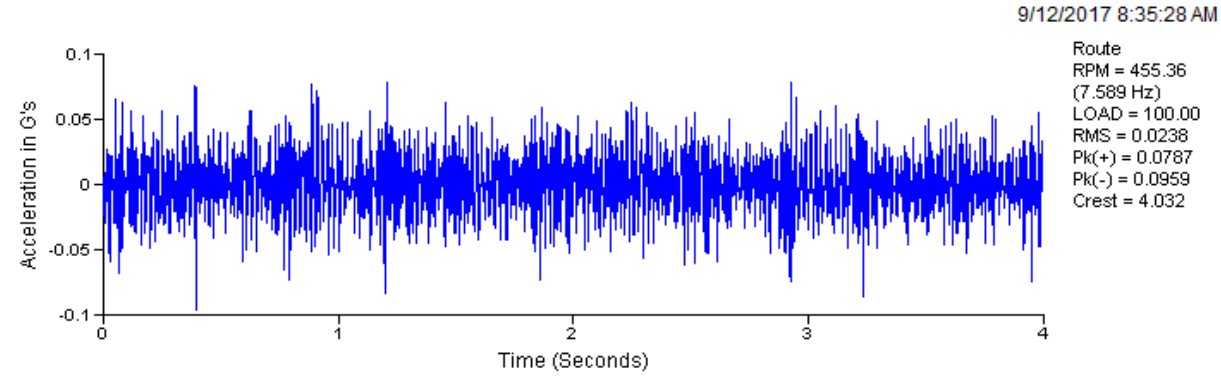

milling.rbm / DEM / Stand 4 / GH3 - Gearbox Horizontal 3

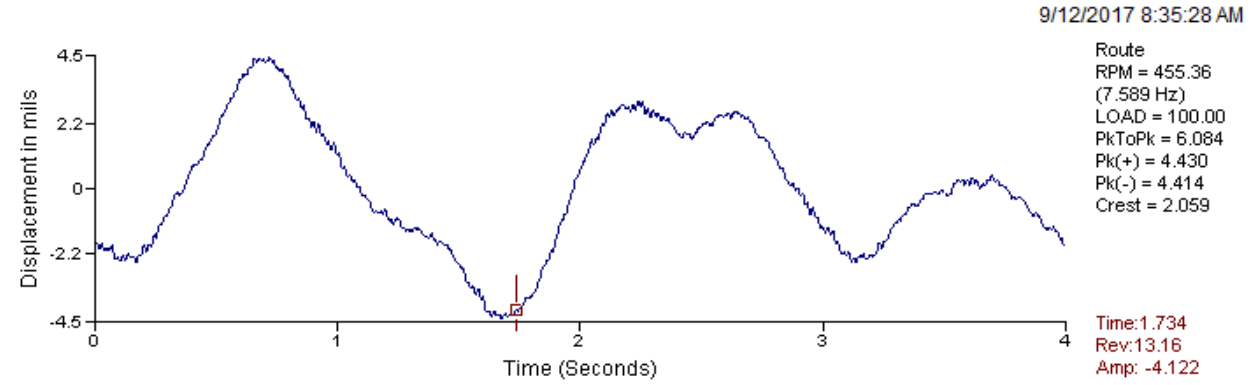

After replacement readings.
Axial vibration readings. Velocity, acceleration, and displacement at lower levels than before.

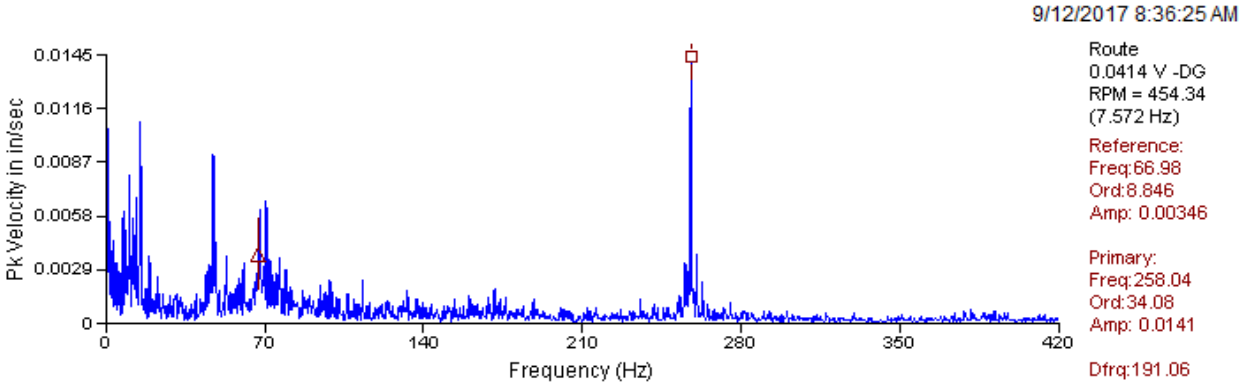

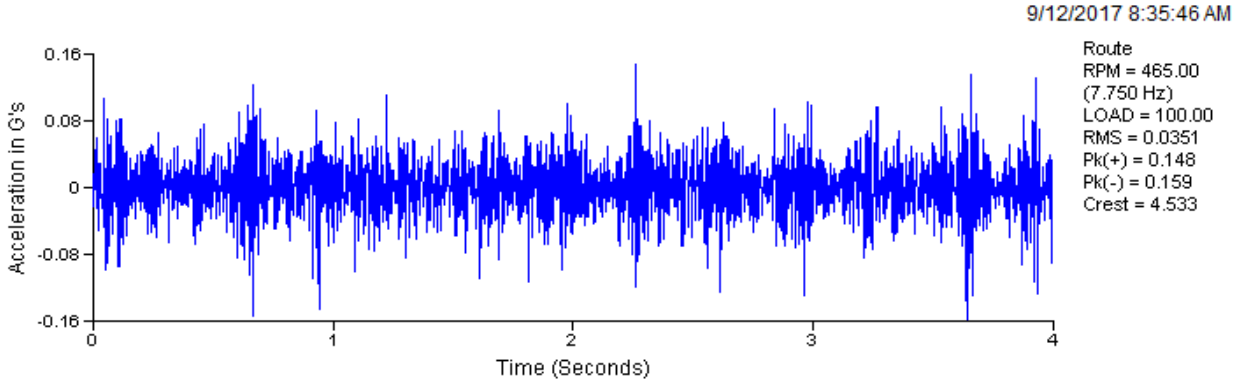

milling.rbm / DEM / Stand 4 / GA3 - Gearbox Axial 3

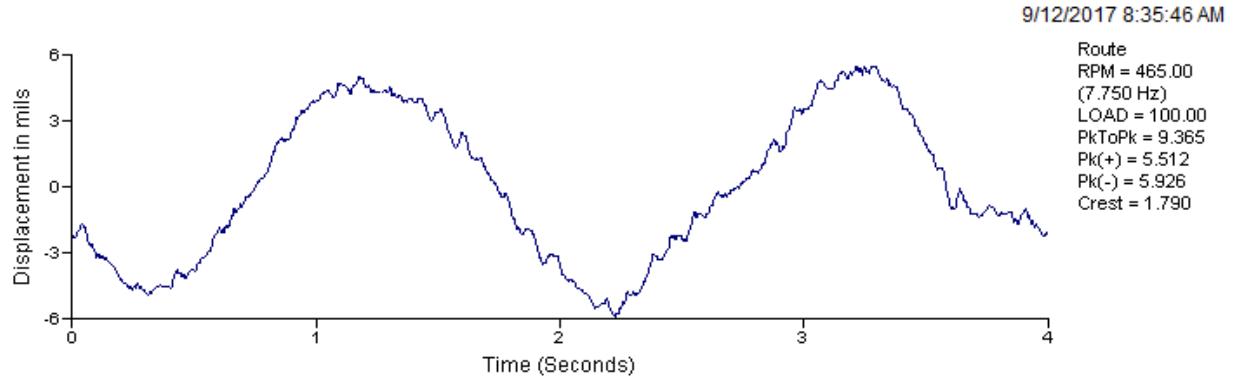

Appendix D – Gearbox 5 Case of Study.
Before replacement readings.
Horizontal vibration readings.

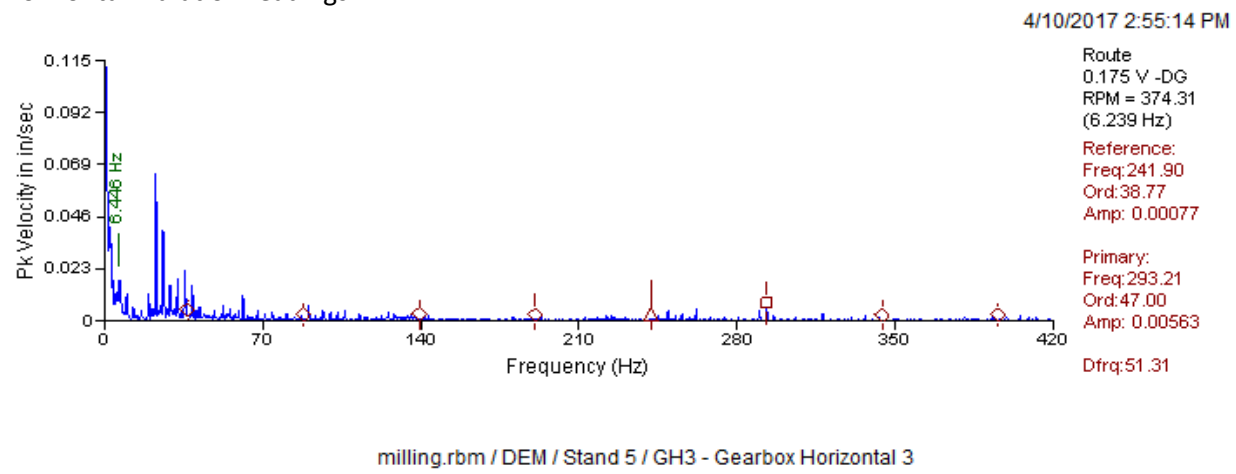

milling.rbm / DEM / Stand 5 / GH3 - Gearbox Horizontal 3

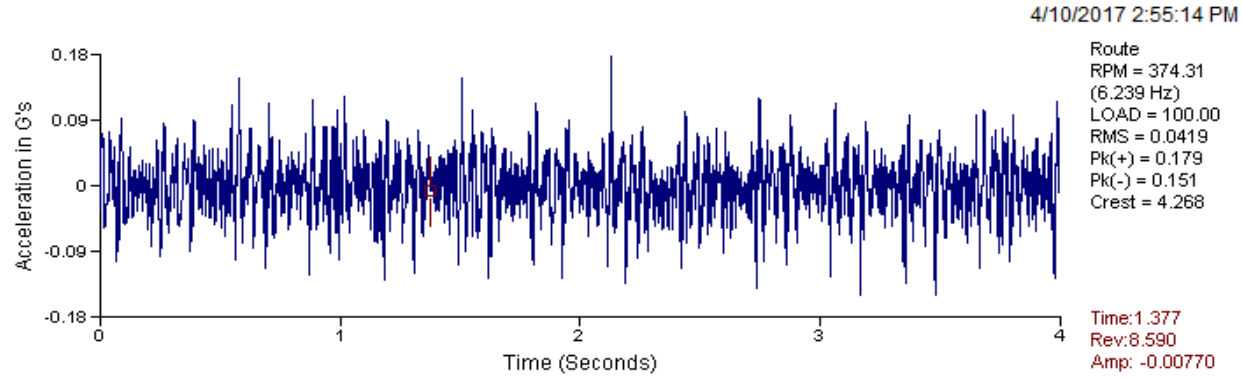

milling.rbm / DEM / Stand 5 / GH3 - Gearbox Horizontal 3

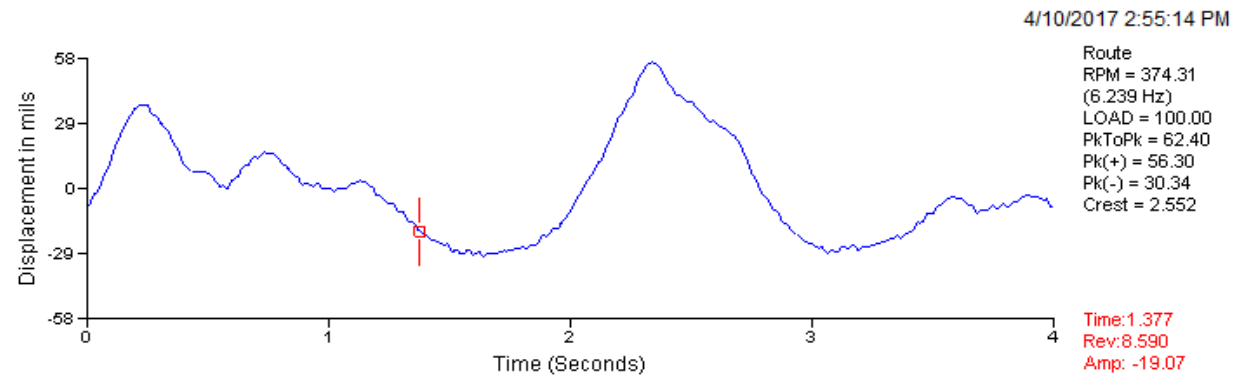

Before replacement readings.
Axial vibration readings. Velocity, acceleration and displacement are respectively below.
Looseness pattern is observed on velocity spectrum.

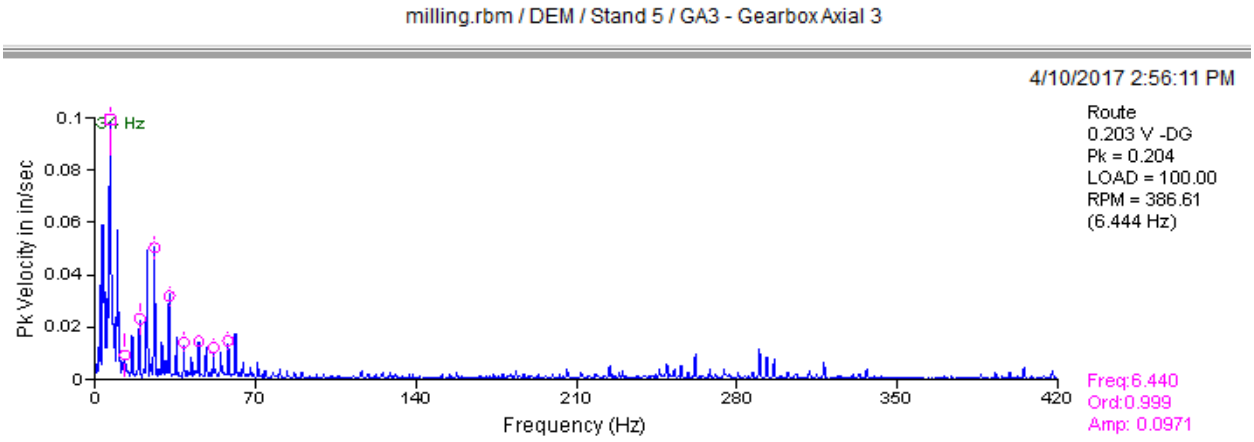

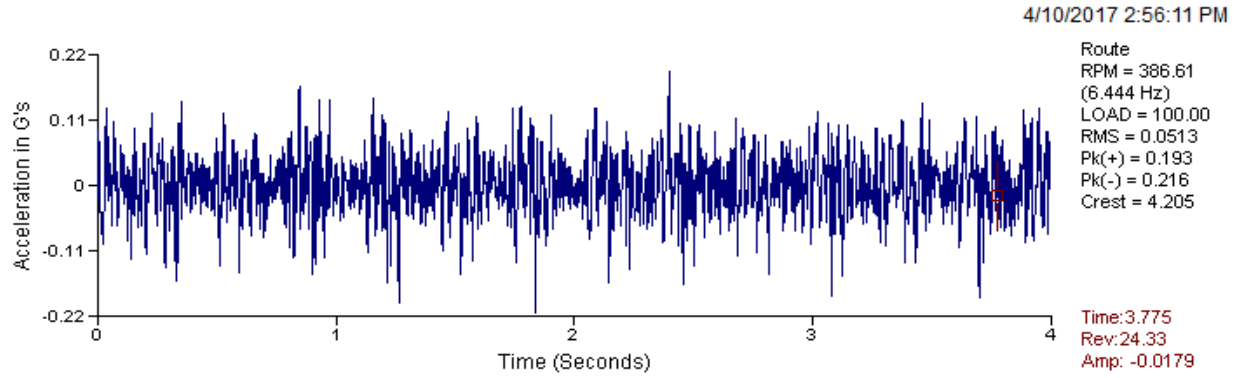

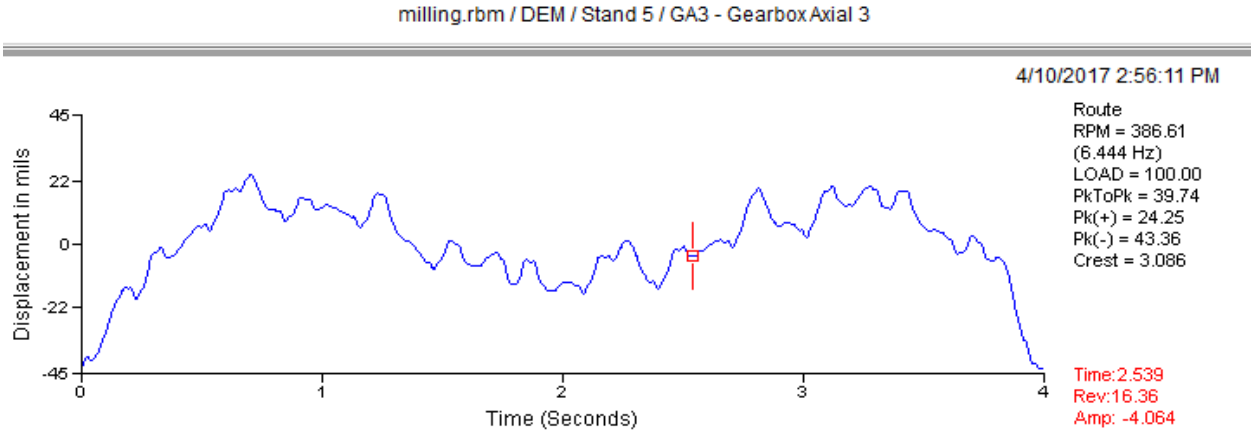

After replacement readings.
Horizontal vibration readings.
Velocity level was reduced by 80%.

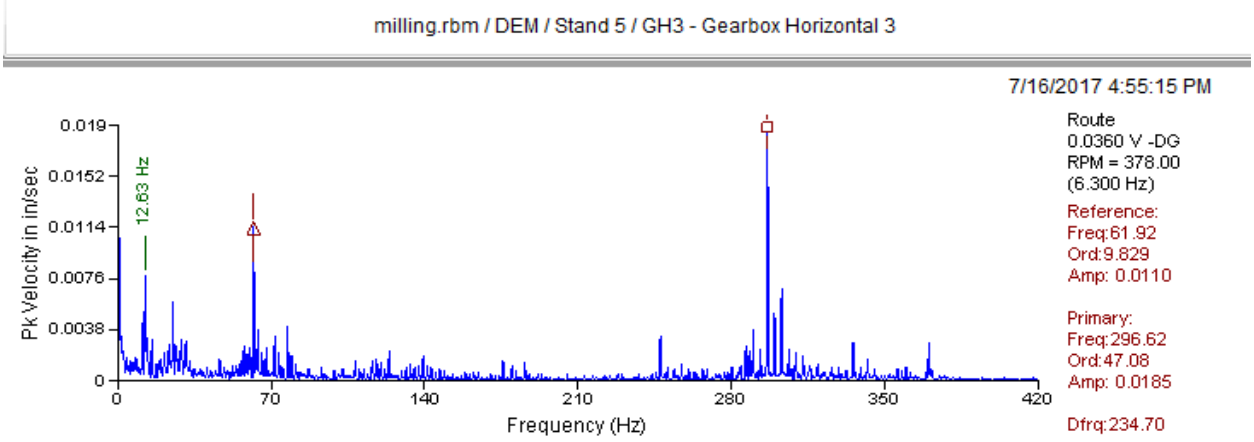

Acceleration.

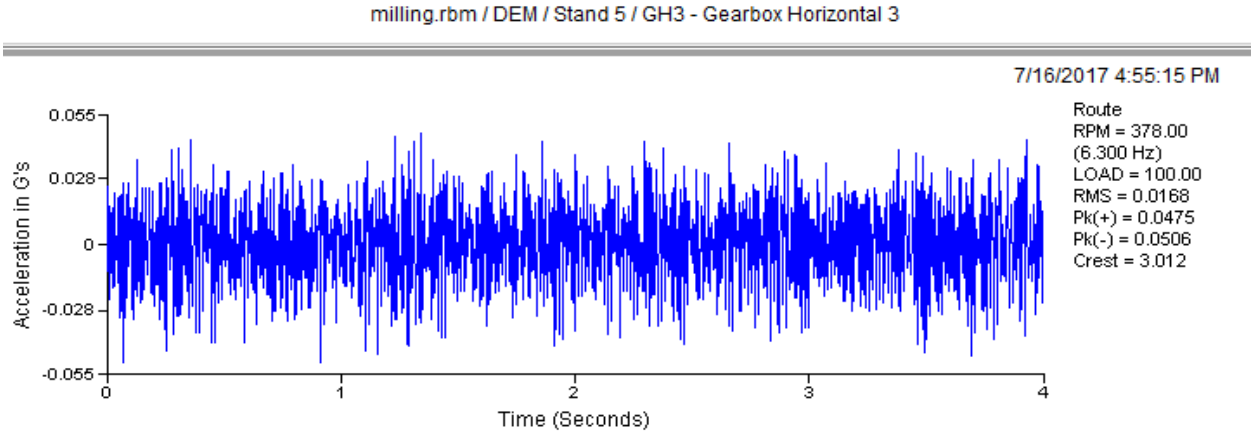

Displacement.

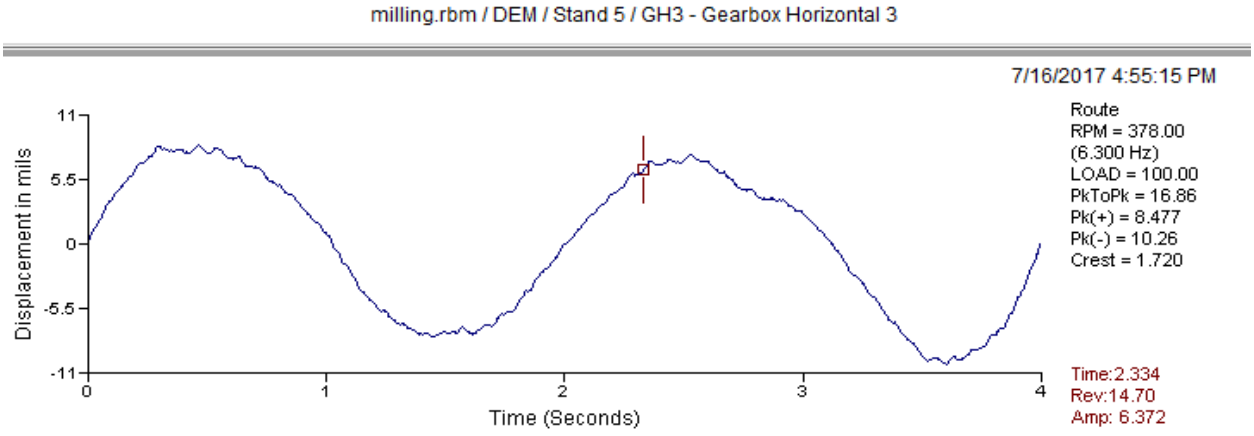

After replacement readings.
Axial vibration readings.

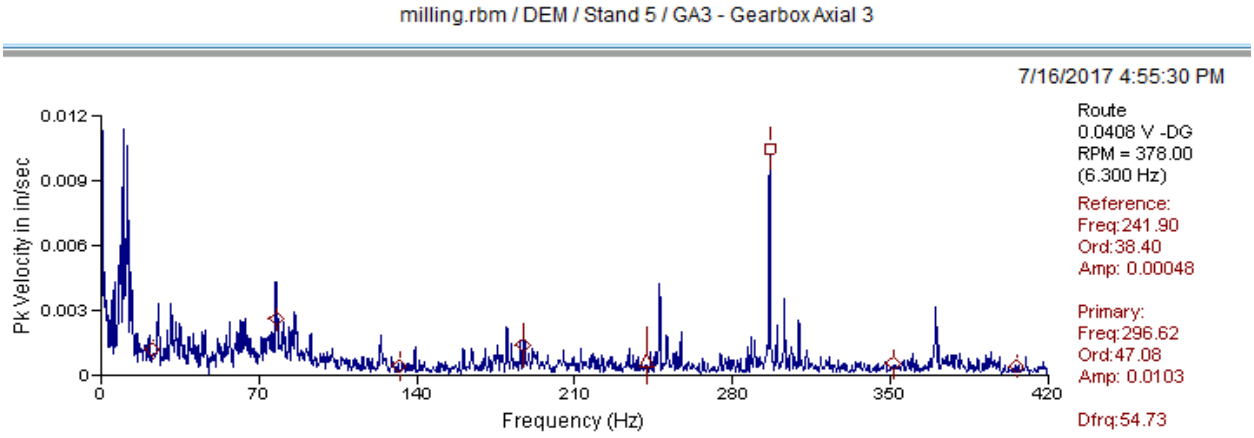

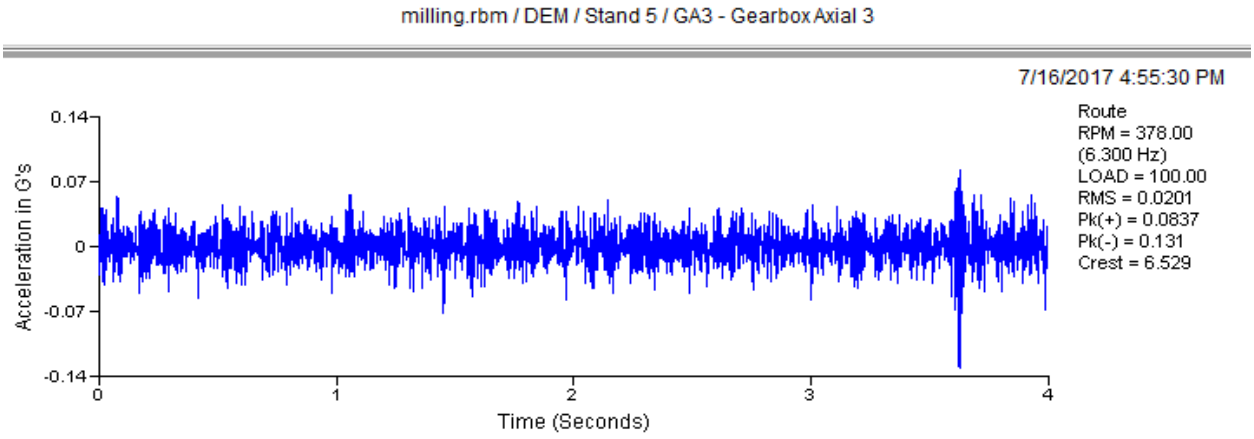

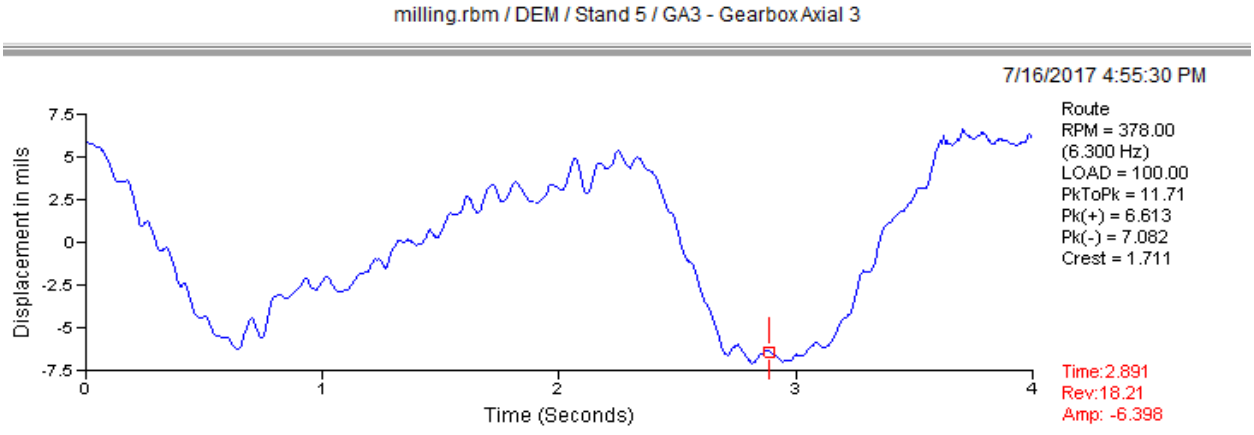

VITA

I am Jesus Gabriel Garcia and I obtained my Bachelor's degree in Mechanical Engineering at UTEP on May 2013. I started working at the steel industry on 2014 with Arcelor Mittal at Vinton, Tx that subsequently became Vinton Steel. I am part of the Maintenance department by applying predictive maintenance techniques with a hgh interest in Materials Science and Engineering in the fields of failure and steels.